viviridae family, encodes the viral structural proteins Core, E1, E2, and p7, as well as six nonstructural proteins (8, 9). Two *N*-glycosylated envelope proteins E1 and E2 are exposed on the surface of the virus and are necessary for viral entry.

The aim of this study was to investigate whether the ERAD pathway is activated upon HCV infection and whether this affects the quality control of virus glycoproteins and virion production. We show that HCV infection triggers the ERAD pathway, possibly through IRE1-mediated splicing of XBP1. Moreover, EDEM1 and EDEM3, but not EDEM2, interact with HCV glycoproteins, resulting in increased ubiquitylation. EDEM1 knockdown and chemical inhibition of the ERAD pathway increases glycoprotein stability, as well as production of infectious virus particles, whereas overexpression of EDEM1 decreases virion production. These results provide insight into the mechanism by which HCV triggers the ERAD pathway and subsequently affects the quality control of virus glycoproteins and virus particle production.

EXPERIMENTAL PROCEDURES

Cell Culture and Chemicals—Human hepatoma cells HuH-7 and HuH-7.5.1 (a gift from Dr. F. V. Chisari (The Scripps Research Institute) (10) and human embryonic kidney cells 293T were cultured at 37 °C and 5% CO_2 in DMEM containing 10% FBS, 10 mM HEPES, 1 mM sodium pyruvate, nonessential minimum amino acids, 100 units/ml penicillin, and 100 μg/ml streptomycin. Tunicamycin (TM) was purchased from Sigma-Aldrich, and kifunensine (KIF) was purchased from Toronto Research Chemicals (Ontario, Canada).

Preparation of Virus Stock—HCV JFH-1 was generated by introducing *in vitro* transcribed RNA into HuH-7.5.1 cells by electroporation, and virus stocks were prepared by infecting at a multiplicity of infection (m.o.i.) of 0.01, as described previously (10). Infected cells were grown in culture medium containing 2% FBS, and supernatants were collected after multiple passages to get high titer virus. The supernatants were concentrated using a 500-kDa hollow fiber module (GE Healthcare) resulting in ~90% recovery of the virus. Focus-forming units were measured with an anti-HCV core antibody to determine virus titration (2H9, described below). Virus stocks containing 1×10^7 focus-forming units/ml were divided into small aliquots and stored at −80 °C until use. rAT strain of Japanese encephalitis virus (JEV) (11) was used to generate virus stock.

Plasmids—cDNAs of mouse EDEM1-HA, EDEM2, and EDEM3-HA, having 92, 93, and 91% amino acid homology with their human orthologs, respectively, were a kind gift from Drs. N. Hosokawa (Kyoto University) and K. Nagata (Kyoto Sangyo University). A HA tag was attached to the C terminus of EDEM2 by PCR, and sequencing analysis was performed to confirm the sequence. To generate pJFH/E1dTM-myc and pJFH/E2dTM-myc, HCV E1 encoding amino acids 170–352 and HCV E2 encoding amino acids 340–714 of JFH-1 polyprotein were amplified by PCR with forward primer and reverse primer containing NotI and XbaI restriction sites, respectively, and cloned into a NotI/XbaI site of the pEF1/Myc-His plasmid (Invitrogen). The pCAGC105E plasmid carrying PrM and E proteins of the rAT strain of JEV has been described (12). Plasmids carrying the firefly luciferase reporter gene under control of the intact promoter of GRP78 and GRP94 or the defective promoter lacking ERSE elements have been described (13) and were a kind gift from Dr. K. Mori (Kyoto University).

Antibodies—Rabbit polyclonal antibodies included anti-HA (Sigma-Aldrich), anti-HCV NS5A (14), anti-SEL1L (Sigma-Aldrich), anti-ubiquitin (MBL, Nagoya, Japan), and anti-JEV E antibodies. The mouse monoclonal antibodies were anti-HA (clone 16B12; Covance, Emeryville, CA), anti-HCV E2 (clone 8D10-3),[3] anti-β-actin (clone AC15; Sigma-Aldrich), anti-HCV core (clone 2H9) (15), and anti-Myc (clone 9E10; Santa Cruz Biotechnology, Santa Cruz, CA) antibodies. Anti-JEV antibodies have been described (16) and were a kind gift from Drs. C. K. Lim and T. Takasaki (National Institute of Infectious Diseases).

Analysis of XBP1 Splicing—Total RNA was extracted from cells using Isogen (Nippon Gene, Tokyo, Japan) following the manufacturer's protocol, and 2 μg of RNA was subjected to cDNA synthesis using oligo(dT) and Superscript III (Invitrogen). PCR was carried out using specific primers 5′-AAACAGAGTAGCAGCTCAGACTGC-3′ and 5′-GTATCTCTAAGACTAGGGGCTTGGTA-3′ for XBP1 and 5′-TCCTGTGGCATCCACGAAACT-3′ and 5′-GAAGCATTTGCGGTGGACGAT-3′ for β-actin to generate PCR fragments of 598 bp for unspliced XBP1, 572 bp for spliced XBP1, and 315 bp for β-actin. The following cycling conditions were used to amplify the genes: 1 cycle of 98 °C for 3 min, followed by 30 cycles of 98 °C for 20 s, 55 °C for 30 s, and 72 °C for 1 min, followed by a final extension of 72 °C for 10 min. The PCR product of XBP1 was further digested with PstI enzyme (New England Biolabs) and resolved on a 2% agarose gel prepared in TAE buffer. Unspliced XBP1 yielded two smaller fragments of 291 and 307 bp whereas spliced XBP1 stayed intact due to loss of the restriction site after splicing.

Gene Microarray Analysis—For microarray analysis, RNA was extracted from HuH-7.5.1 cells at 48 and 72 h after JFH-1 infection. Cells treated for 12 h with 5 μg/ml TM served as a positive control. Hybridization was performed on a 3D-Gene (see 3D-Gene web site) Human Oligonucleotide chip 25k (Toray Industries Inc., Tokyo, Japan). For efficient hybridization, this microarray chip has three dimensions and is constructed with a well between the probes and cylinder stems with 70-mer oligonucleotide probes on the top. Total RNA was labeled with Cy3 or Cy5 using the Amino Allyl MessageAMP II aRNA Amplification kit (Applied Biosystems). The Cy3- or Cy5-labeled aRNA pools were subjected to hybridization for 16 h using the supplier's protocol. Hybridization signals were scanned using a ScanArray Express Scanner (PerkinElmer Life Sciences) and processed by GenePixPro version 5.0 (Molecular Devices, Sunnyvale, CA). Detected signals for each gene were normalized using a global normalization method (Cy3/Cy5 ratio median = 1). Genes with Cy3/Cy5 normalized ratios $>\log_2 1.0$ or $<\log_2 -1.0$ were defined, respectively, as significantly up- or down-regulated genes.

Quantification of Cellular Gene Expression—Gene expression levels were measured using predesigned assay-on-demand (Applied Biosystems). RT-PCR amplification was performed

[3] D. Akazawa, N. Nakamura, and T. Wakita, unpublished data.

under the following conditions: 48 °C for 30 min, 95 °C for 10 min, 50 cycles of 95 °C for 15 s, and 60 °C for 1 min. Standard curves were constructed on a 1:5 serial dilution of the RNA template. The results were normalized to GAPDH mRNA levels.

Determination of Protein Stability—HuH-7 cells were infected with HCV JFH-1 at a m.o.i. of 2. Six hours after infection, the cells were either treated with KIF or transfected with EDEM1 siRNA. Forty hours later, culture medium was replaced with 100 μg/ml cycloheximide (CHX). Cells, including floating cells, were harvested at different time points after CHX addition, and immunoblotting was performed to determine the amount of HCV E2.

Plasmid Transfection and Immunoprecipitation—HuH-7 or 293T cells were seeded in 6-well cell culture plates at 3×10^5 cells/well and cultured overnight. Plasmid DNA was transfected into cells using TranIT-LT1 transfection reagent (Mirus, Madison, WI). Cells were harvested at 48 h after transfection, washed once with 1 ml of PBS, and lysed in 200 μl of lysis buffer (20 mM Tris-HCl, pH 7.4, 135 mM NaCl, 1% Triton X-100, and 10% glycerol supplemented with 50 mM NaF, 5 mM Na_3VO_4, and protease inhibitor mixture tablets (Roche Diagnostics). Cell lysates were sonicated at 4 °C for 10 min, incubated for 30 min at 4 °C, and centrifuged at 14,000 × *g* for 5 min at 4 °C. After preclearing for 2 h, the supernatants were immunoprecipitated overnight by rotating with 1.5 μl of anti-HA monoclonal antibody (16B12) or anti-HCV E2 monoclonal antibody (clone 8D10-3) at 4 °C. The immunocomplexes were then captured on protein G-agarose beads (Invitrogen) by rotation-incubation at 4 °C for 3 h. Beads were subsequently precipitated by centrifugation at 800 × *g* for 1 min and washed five times with lysis buffer. Finally, proteins bound to the beads were boiled in 40 μl of SDS sample buffer and subjected to SDS-PAGE.

Western Blotting—Proteins resolved by SDS-PAGE were transferred onto PVDF membranes (Immobilon; Millipore). After blocking in 2% skim milk, the membranes were probed with primary antibodies followed by exposure to peroxidase-conjugated secondary antibodies and visualization with an ECL Plus Western blotting detection system (GE Healthcare). The intensity of the bands was measured using a computerized imaging system (ImageJ software; National Institutes of Health).

Small Interfering RNA (siRNA) Transfection—HuH-7 cells were transfected with duplex siRNAs at a final concentration of 10 nM using Lipofectamine RNAiMAX (Invitrogen). Three siRNAs for each gene were examined for knock-down efficiency and cytotoxic effects. The siRNA with best performance was selected for further experiments. Target sequences of the siRNAs which exhibited the best knock-down efficiencies were as follows: EDEM1 (sense) 5′-CAUAUCCUCGGGUGAAUCUtt-3′, EDEM2 (sense) 5′-GAAUGUCUCAGAAUUCCAAtt-3′, EDEM3 (sense) 5′-CAUGAGACUACAAAUCUUAtt-3′, IRE1 (sense) 5′-GGACGUGAGCGACAGAAUAtt-3′. 5′-GGUGUCCUUACCAUACUAAtt-3′ served as a negative control. The lowercase letters denote overhanging deoxyribonucleotides.

Quantification of HCV Core and RNA—HCV core was quantified using an enzyme immunoassay (Ortho HCV antigen ELISA kit; Ortho Clinical Diagnostics, Tokyo, Japan). HCV RNA was quantified as described (17).

Statistical Analysis—Student's *t* test was employed to calculate the statistical significance of the results. $p < 0.05$ was considered significant.

RESULTS

HCV Infection Induces XBP1 mRNA Splicing and EDEM Expression—XBP1 plays a key role in activating the ERAD pathway, which mediates unfolded protein response in the ER. Under conditions of ER stress, XBP1 mRNA is processed by unconventional splicing and translated into functional XBP1, which in turn mediates transcriptional up-regulation of a variety of ER stress-dependent genes. The resultant activation of downstream pathways boosts the efficiency of ERAD, which coincides with elevated transcription of EDEMs. To validate our method for detecting activation of the ERAD pathway, we exposed HuH-7.5.1 cells to TM, which is a typical ER stress inducer, and performed an assay to quantify spliced XBP1 mRNA, as described under "Experimental Procedures," at different time points after treatment. The spliced form of XBP1 mRNA started accumulating within these cells as early as 2 h after exposure to TM (Fig. 1*A*), and levels remained elevated until at least 12 h after treatment. Quantitative RT-PCR showed that mRNA levels of EDEM1, EDEM2, and EDEM3 were elevated in TM-treated cells whereas ER ManI, which is not an ER stress-responsive gene, did not show any up-regulation (Fig. 1*B*). To examine involvement of the ERAD pathway in the HCV life cycle, we infected HuH-7.5.1 cells with JFH-1 at m.o.i. of 5 and analyzed XBP1 mRNA splicing and EDEM up-regulation. Upon infection, the fragment corresponding to spliced XBP1 mRNA, was detectable 8 h after infection, and the difference in splicing between mock- and HCV-infected cells became more pronounced at 48 h after infection and then persisted (Fig. 1*C*). Increased levels of XBP1 mRNA splicing were dependent on the m.o.i. (supplemental Fig. 1*A*), suggesting that expression of active XBP1 was induced by HCV infection. A small amount of spliced XBP1 was detected in mock-infected cells, presumably because of some intrinsic stress. A 3.1-fold increase in the level of EDEM1 mRNA was observed at 3–4 days after infection ($p < 0.05$). Increases in EDEM2 and EDEM3 mRNA levels were moderate and reached ~1.5-fold, whereas ER ManI mRNA exhibited no change after infection (Fig. 1*D*). Expression of EDEMs, particularly EDEM1, was up-regulated in accordance with HCV infection titers (supplemental Fig. 1*B*). Knocking down the IRE1 gene (Fig. 1*E*) effectively reversed the accumulation of spliced XBP1, as well as the transcriptional up-regulation of EDEM1 (Fig. 1*F*), thus confirming that HCV infection induces ERAD through the IRE1-XBP1 pathway.

To enable a comprehensive investigation of the transcriptional changes that occur, up- and down-regulation of the transcriptome was examined in HCV-infected cells and in TM-treated cells. The results were compared with those of mock-transfected cells at each time point. A range of genes involved in ER stress was found to be regulated in HCV-infected and in TM-treated cells (Fig. 2*A*). EDEM1 was signifi-

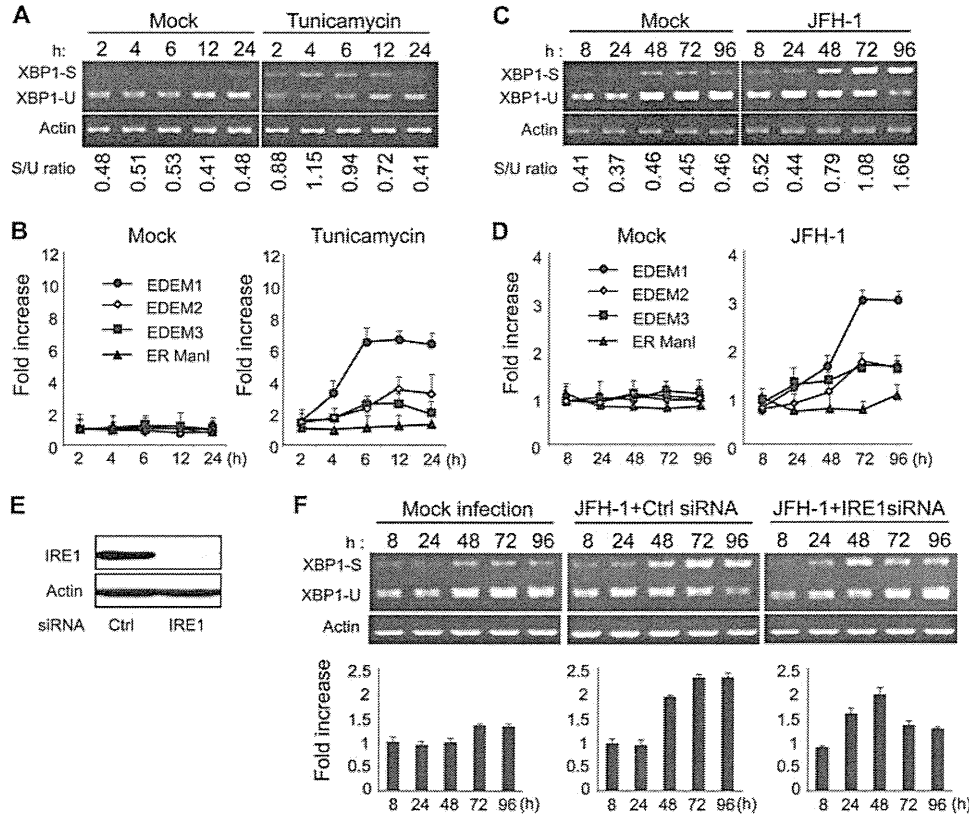

FIGURE 1. **Splicing of XBP1 mRNA and induction of ERAD gene expression in HCV JFH-1-infected cells.** *A*, splicing of XBP1 mRNA analyzed in mock- and TM (5 μg/ml)-treated HuH-7.5.1 cells at different time points after treatment. The *upper* and *lower bands* represent spliced and unspliced RNA, respectively. The *numbers* at the *bottom* of the *panel* indicate the density ratios of bands corresponding to spliced and unspliced XBP1. *B*, graphs showing the -fold induction of EDEM1, EDEM2, EDEM3, and ER Man1 mRNA in HuH-7.5.1 cells treated or untreated with TM. Data are normalized to GAPDH expression levels. The mean ± S.D. (*error bars*) of three independent experiments are shown. *C*, splicing of XBP1 mRNA analyzed in mock- and HCV JFH-1-infected HuH-7.5.1 cells (m.o.i. 5) at different time points after infection. *Numbers* at the *bottom* of the *panel* indicate the density ratios of bands corresponding to spliced and unspliced XBP1. *D*, real-time PCR analysis of EDEM1, EDEM2, EDEM3, and ER ManI mRNA induction in mock- and HCV-infected cells. Data are normalized to GAPDH expression. The mean ± S.D. of three independent experiments are shown. Note that a reduction in the level of GAPDH mRNA within infected cells was not observed until 96 h after infection when a slight decrease was observed. This led us to use GAPDH as a housekeeping gene in our experiments. *E*, Western blotting of IRE1 in cells transfected with mock or gene-specific siRNA of IRE1. *F*, splicing of XBP1 mRNA and induction of EDEM1 in HCV-infected cells after knocking down of the IRE1 gene. HuH-7.5.1 cells infected with JFH-1 at a m.o.i. of 5 were transfected with mock (*center*) or IRE1-specific siRNA (*right*) 48 h after infection, after which splicing of XBP1 (*upper*) and transcriptional up-regulation of EDEM1 (*lower*) were examined at the indicated time points after infection. The mean ± S.D. of two independent experiments are shown.

cantly up-regulated upon HCV infection, whereas expression levels of EDEM2 and EDEM3 remained unchanged. Although transcriptional changes caused by HCV infection in many of the genes listed are analogous to those that occur in cells treated with TM, up-regulation of two ER chaperone proteins, GRP78 and GRP94, was induced by TM treatment but not by HCV infection. This differential induction was confirmed by a reporter assay for GRP78 promoter and GRP94 promoter activities (Fig. 2*B*). These results are in agreement with a previously described finding that GRP78 and GRP94 are not responsive to HCV infection in hepatoma cells (18). It remains likely that HCV infection interferes with transcriptional activation of some ER chaperone proteins; however, the mechanism by which this occurs remains to be elucidated.

EDEMs Cause Ubiquitylation of HCV Glycoproteins and Enhance Their Degradation—Because EDEMs have been reported to enhance proteasomal degradation of ERAD substrates through direct binding, we investigated the interaction of EDEMs with HCV glycoproteins in 293T cells by co-transfecting the expression plasmids for E1dTM or E2dTM together with plasmids carrying either EDEM or ER ManI genes. Immunoprecipitation and immunoblotting demonstrated that each EDEM, but not ER ManI, was capable of interacting with E2 (Fig. 3*A*) and E1 (supplemental Fig. S2). HCV glycoproteins displayed enhanced mobility when co-expressed with EDEM1, EDEM3, or ER ManI, which could be due to the mannosidase activity of these proteins, which is lacking in EDEM2 (6). HCV primarily replicates in hepatocytes so we examined the interaction of EDEMs with E2dTM in HuH-7 cells as well, which yielded similar results (data not shown). E2dTM lacks the transmembrane domain, which could affect its folding and ER retention and thus modulate the ability of this protein to interact with EDEMs and ER ManI. Second, E1 and E2 glycoproteins assemble as noncovalent heterodimers to make functional complexes, which may alter the interaction of these proteins with EDEMs. To address these issues, we co-transfected HuH-7 cells with plasmids carrying full-length E1E2 glycoproteins together with plasmids carrying either EDEMs or ER ManI. Similar phenotypes were produced following transfection full-length E1E2 proteins (supplemental Fig. S3*A*), demonstrating that functional complexes of HCV glycoproteins bind with EDEMs. Recently, we have reported on the development of a

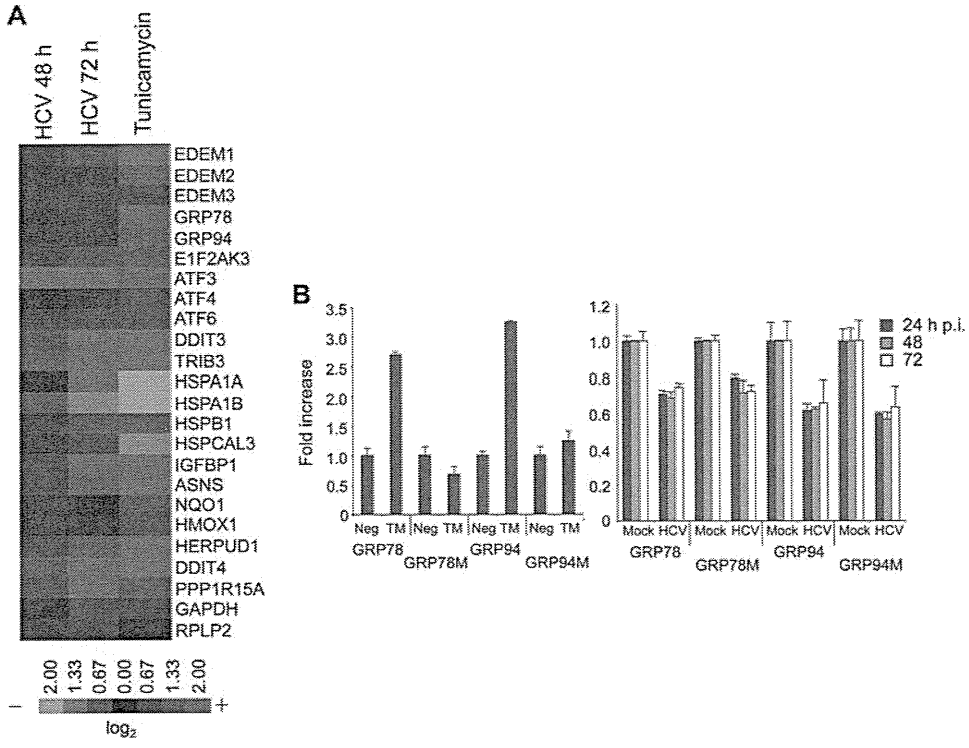

FIGURE 2. **Comprehensive analysis of ERAD gene expression in JFH-1-infected HuH-7.5.1 cells.** *A*, HuH-7.5.1 cells treated with TM (5 μg/ml) for 12 h or infected with JFH-1 for 48 and 72 h were subjected to microarray analysis, along with their negative controls. Expression of ER stress genes is shown as a heat map. *Red* and *green* indicate up- and down-regulation, respectively. Information on each gene shown is indicated on the 3D-Gene web site. *B*, GRP78 and GRP94 induction in TM-treated (*left*) and HCV-infected cells (*right*). GRP78M and GRP94M represent the defective promoters. The mean ± S.D. (*error bars*) of three independent experiments are shown.

packaging system of HCV subgenomic replicon sequences through the provision of viral core NS2 proteins in *trans* (19). Transcomplementation with core NS2 proteins resulted in successful packaging of the viral sequences; therefore, plasmids carrying these proteins are a valid construct by which to examine the interaction of envelope proteins with ERAD machinery. Thus, we performed an immunoprecipitation assay of HuH-7 cells co-transfected with core NS2 and EDEMs. In agreement with our previous results, EDEMs, but not ER ManI, were observed to bind to HCV E2 protein (supplemental Fig. S3*B*). To examine the functional importance of this interaction, we analyzed the ubiquitylation of HCV E2 protein in cells co-transfected with HCV E2 and EDEM proteins. An immunoprecipitation assay revealed that overexpression of EDEM1 and EDEM3, but not of EDEM2 and ER ManI, dramatically increased the ubiquitylation of HCV glycoprotein (Fig. 3*B*). In mammals, the ER membrane ubiquitin-ligase complex involved in the dislocation of ERAD substrates, and their ubiquitylation contains the ER membrane adaptor SEL1L. It has recently been shown that SEL1L interacts with EDEM1 in cells and functions as a cargo receptor for ERAD substrates (20); however, it is unknown whether SEL1L interacts with other EDEMs. We therefore assessed whether SEL1L interacts with EDEM1, EDEM2, EDEM3, and ER ManI in cells (Fig. 3*C*). Interestingly, endogenous SEL1L co-precipitated with EDEM1 and EDEM3, whereas little to no interaction was observed with EDEM2 and ER ManI. Collectively, it is likely that, although all EDEMs can recognize HCV E1 and E2, EDEM1 and EDEM3 are involved in the ubiquitylation of HCV glycoproteins by delivering them to SEL1L-containing ubiquitin-ligase complexes. To investigate further the role of EDEMs in quality control of HCV glycoproteins, we measured the steady-state level of HCV E2 protein after EDEM knockdown. Transfection of HCV-infected cells with siRNAs against EDEM1, EDEM2, or EDEM3 caused a 60–80% reduction in mRNA levels of the respective genes (Fig. 3*D*) with no cytotoxic effects observed (data not shown). Immunoblotting showed a considerable increase in the steady-state level of viral E2 in EDEM1 siRNA-treated cells (Fig. 3*D*). We subsequently examined the turnover of E2 in cells with and without EDEM1 knockdown. In CHX half-life experiments, E2 protein was moderately unstable in control-infected cells, presumably via proteasomal degradation (Fig. 3*E*). Treatment with MG132, a proteasome inhibitor, blocked its destabilization (data not shown). In contrast, E2 was completely stable in EDEM1-knockdown cells during the chase period of time tested (Fig. 3*E*). Together, these results strongly suggest that EDEM1 and EDEM3, particularly EDEM1, are involved in the post-translational control of HCV glycoproteins.

Involvement of EDEM1 in the Production of Infectious HCV—Given the involvement of EDEMs in the turnover of HCV glycoproteins, we investigated whether EDEMs affect the replication and production of infectious virus particles. EDEMs were knocked down in HCV-infected HuH-7 cells by siRNA transfection, and the production of infectious particles was then monitored by measuring the extracellular infectivity titer. Knocking down of EDEM1 and EDEM3 in the infected cells resulted in ~3.1-fold ($p < 0.05$) and ~2.3-fold increases in virus production, respectively, compared with control cells. No effect

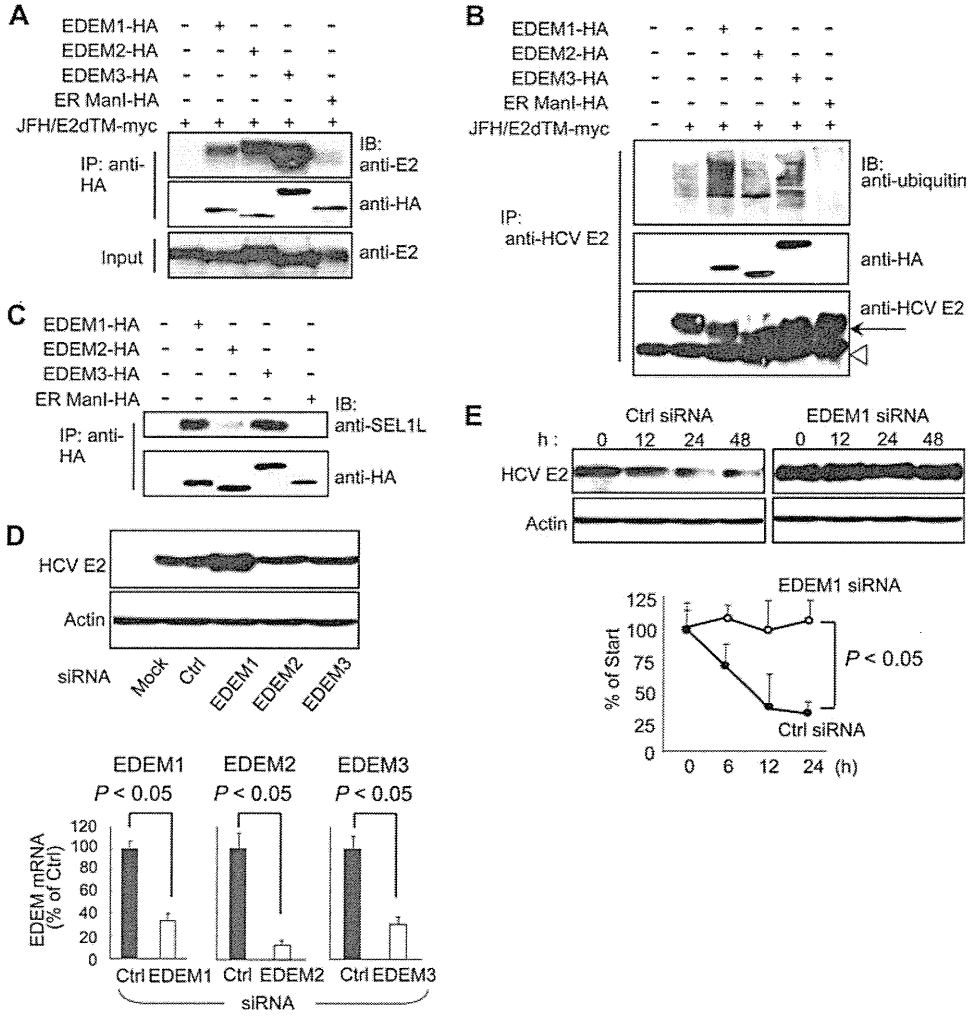

FIGURE 3. **EDEMs are involved in the degradation of HCV glycoproteins.** *A*, binding of EDEMs and ER ManI with HCV E2. 293T cells were seeded in 6-well plates at a density of 3×10^5 cells/well. After overnight incubation, cells were co-transfected with plasmids carrying HCV E2-myc (1 μg) and EDEM1-HA, EDEM2-HA, EDEM3-HA, or ER ManI-HA proteins (1 μg each). Forty-eight hours later, cells were harvested, immunoprecipitated (*IP*) with anti-HA antibodies, and Western blotting (*IB*) was performed with the indicated antibodies. *B*, ubiquitylation of HCV E2 protein in cells co-transfected with HCV E2 and EDEM plasmids. 293T cells were seeded in 6-well plates at a density of 3×10^5 cells/well. Twenty-four hours later, the cells were co-transfected with plasmids carrying HCV E2-myc (1 μg) and EDEM1-HA, EDEM2-HA, EDEM3-HA, or ER ManI-HA genes (1 μg each). Forty-eight hours later, the cells were harvested and immunoprecipitated with anti-E2 antibodies, and Western blotting was performed with the indicated antibodies. *Arrow*, HCV E2; *open arrowhead*, immunoglobulin heavy chain. *C*, binding of EDEMs and ER ManI with endogenous SEL1L in cells. *D*, steady-state level of HCV E2 in HCV-infected HuH-7 cells after EDEM knockdown (*upper*). The knockdown efficiencies of the respective siRNAs are shown in the *lower panel*. Values are normalized to GAPDH expression levels, and normalized values in negative control cells have been arbitrarily set at 100%. *E*, stability of HCV E2 protein in EDEM1 knockdown cells. HCV-infected HuH-7 cells were transfected with control or EDEM1 siRNA. Forty hours later, the cells were exposed to CHX (100 μg/ml) for 0, 12, 24, and 48 h, followed by immunoblotting. Specific signals were quantified by densitometry, and the percent of HCV E2 remaining was compared with initial levels. The mean ± S.D. (*error bars*) of two independent experiments are shown.

on virus production was observed following EDEM2 gene silencing (Fig. 4*A*). On the other hand, no significant differences were observed with regard to intracellular HCV core protein levels among mock- and EDEM siRNA-transfected cells (Fig. 4*B*), which indicates that replication of the viral genome is not affected by EDEM proteins. To examine further whether this effect on virus production was due to turnover of HCV envelope proteins, we performed loss-of-EDEM-function experiments in HuH-7 cells carrying HCV subgenomic replicons. Because the replicons do not require envelope proteins, they should be insensitive to the expression levels of genes involved in the ERAD pathway. As expected, siRNA-mediated knockdown of EDEMs resulted in little to no change in genome replication (supplemental Fig. S4*A*). To investigate further the participation of EDEMs in the HCV life cycle, HCV-infected cells were examined 48 h after transfection with an expression plasmid for either EDEM1, EDEM2, or EDEM3. As expected, exogenous expression of EDEM1 in the infected cells led to a 2.4-fold decrease in virus production compared with mock-transfected cells ($p < 0.05$) (Fig. 4*C*). A moderate decrease of 1.7-fold was observed in the cells overexpressing EDEM3 protein. Ectopic expression of EDEMs and ER ManI did not cause any change in intracellular HCV core protein levels (Fig. 4*D*). Similarly, little or no change was observed in genome replication when plasmids carrying EDEMs were introduced into HCV subgenomic replicon cells (supplemental Fig. S4*B*). These results indicate that EDEM1 and EDEM3, particularly EDEM1, regulate virus production, possibly through post-translational control of HCV glycoproteins.

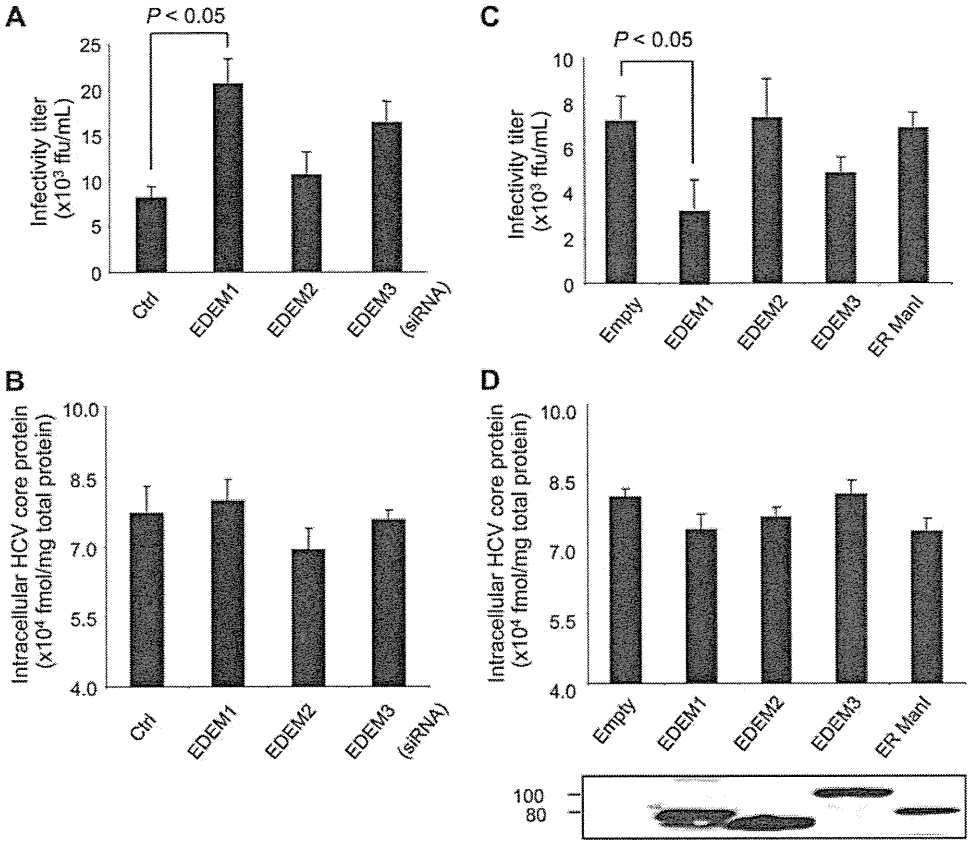

FIGURE 4. **Role of EDEMs in HCV replication and production of infectious virus particles.** *A*, HCV production in HuH-7 cells transfected with EDEM siRNAs. Cells were infected with JFH-1 at a m.o.i. of 1. Twenty-four hours later, the cells were transfected with the indicated siRNAs at a final concentration of 10 nM. The culture medium was harvested 48 h later and was used to infect naïve HuH-7.5.1 cells seeded in a 96-well plate. Immunostaining using anti-HCV core antibodies was performed at 72 h after infection, and focus-forming units were counted. *B*, siRNA-transfected and HCV-infected cells described in *A* harvested at 48 h after infection. Intracellular HCV core protein was measured. The values were normalized to total protein in the cell lysate samples. *C*, HCV production in HuH-7 cells transfected with plasmids carrying EDEM1-HA, EDEM2-HA, EDEM3-HA, or ER ManI-HA genes. *D*, intracellular HCV core protein within the cells described in *C*. Expression levels of the EDEMs and ER ManI were determined by anti-HA immunoblotting. The mean ± S.D. (*error bars*) of three independent experiments are shown in all of the *panels*.

Chemical Inhibition of the ERAD Pathway Increases HCV Production—KIF, a potent inhibitor of ER mannosidase, is reported to inhibit the ERAD pathway. When HCV-infected cells were treated with KIF, virus production increased in the culture medium in a dose-dependent manner (Fig. 5*A*, *left*), and the steady-state level of E2 in the cells increased accordingly (Fig. 5*A*, *right*). No change was observed in intracellular HCV core protein levels after KIF treatment (Fig. 5*A*, *center*). Kinetic analyses showed that E2 was stabilized dramatically in KIF-treated cells (Fig. 5*B*), whereas the fate of HCV core protein, a nonglycoprotein, was not affected by KIF treatment (supplemental Fig. S5). No effect on virus replication was observed when the cells harboring JFH-1 subgenomic replicons were treated with KIF (data not shown).

On the basis of these findings, one may hypothesize that KIF contributes to the stabilization of HCV glycoprotein(s) by interfering with the interaction between (i) EDEMs and viral proteins, or (ii) EDEMs and SEL1L. To address this, HCV E2 was co-expressed in 293T cells with EDEM1, EDEM2, EDEM3, or ER ManI in the presence or absence of KIF, followed by immunoprecipitation (Fig. 5*C*). E2 was shown to interact with EDEM1, EDEM2, and EDEM3, analogous to the data shown in Fig. 3*A*, and KIF did not block the interactions. Decreased electrophoretic mobility of E2 was detected in KIF-treated cells, possibly due to a change in glycan composition caused by inhibition of mannosidase activity. These findings led us to investigate whether the glycans on HCV glycoproteins are required for binding to EDEMs. We generated E1 and E2 mutants by replacing their *N*-glycosylation sites with glutamine residues and analyzed their interaction with EDEMs. Removal of the glycans did not inhibit the binding of E1 and E2 proteins to EDEM, demonstrating that *N*-glycans on the surface of viral proteins are not indispensible for an interaction between EDEMs and HCV glycoproteins to occur (supplemental Fig. S6). The effect of KIF on the association of EDEMs with downstream ERAD machinery was examined further. In cells co-expressing E2 and EDEMs, the interaction of SEL1L with EDEM1 and EDEM3 was significantly reduced in the presence of KIF ($p < 0.05$) (Fig. 5*C*). Consistent with these results, KIF abrogated the EDEM1- and EDEM3-mediated ubiquitylation of HCV E2 protein (Fig. 5*D*). This inhibitory effect of KIF on the SEL1L-EDEM interaction was also observed in HuH-7 cells (supplemental Fig. S7). These results suggest that KIF stabilizes HCV glycoproteins by interfering with the SEL1L-EDEM interaction and thus leads to an increase in virus production.

Role of ERAD in the Life Cycle of JEV—This study demonstrates involvement of the ERAD pathway in HCV production. However, the role of this pathway in the production of other

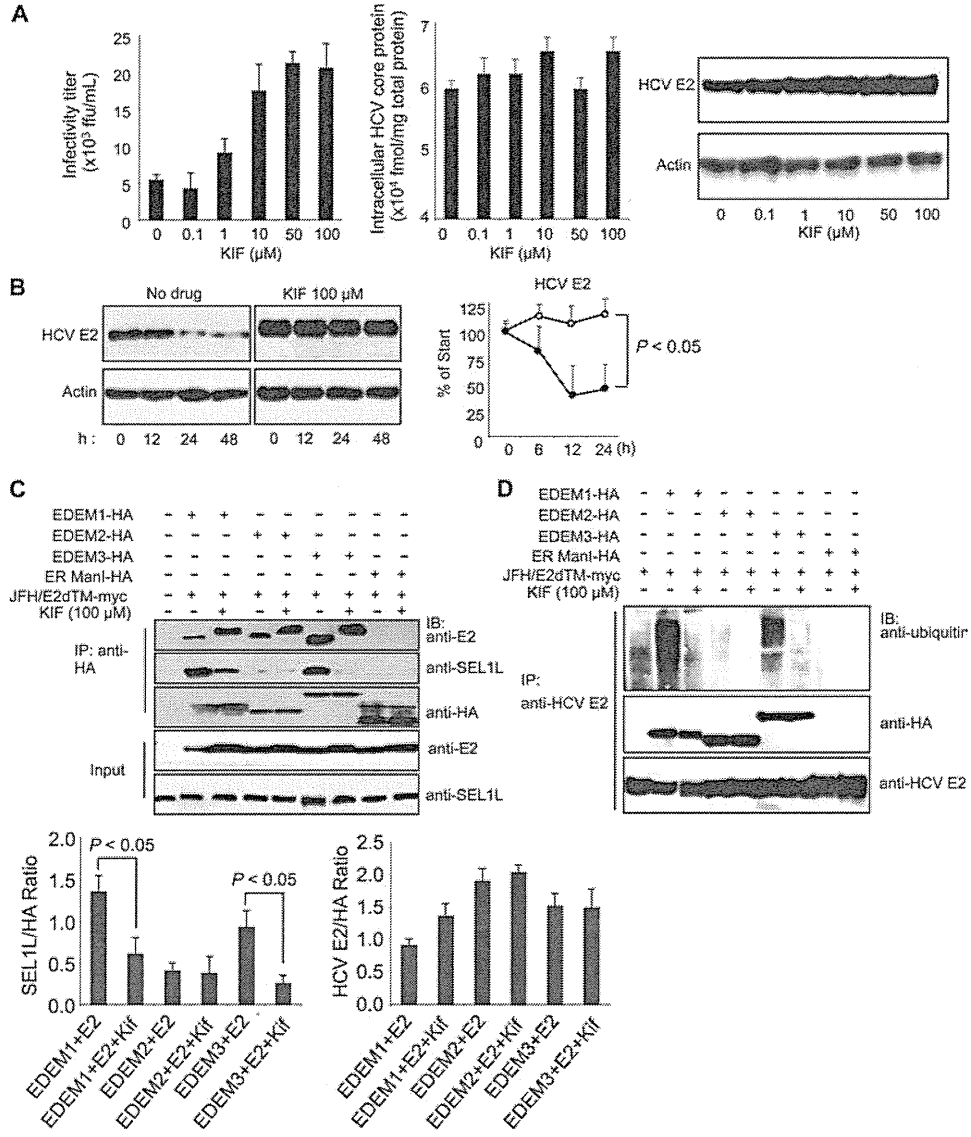

FIGURE 5. **Effect of KIF on HCV production and stability of E2.** *A*, extracellular HCV titer, intracellular HCV core protein expression, and steady-state level of HCV E2 in HuH-7 cells treated with different concentrations of KIF. *B*, CHX-based HCV protein stability assay of HCV E2 protein in KIF-treated cells as described in Fig. 3*E*. E2 protein levels normalized to actin levels are shown in the *graph* on the *right*. The *open* and *filled circles* indicate KIF-treated and nontreated cells, respectively. The mean ± S.D. (*error bars*) of two independent experiments are shown. *C*, binding of EDEMs and ER ManI with HCV E2 and SEL1L in 293T cells in the absence or presence of KIF. 293T cells were seeded in 6-well plates at a density of 3×10^5 cells/well. After overnight incubation, the cells were co-transfected with plasmids carrying HCV E2-myc (1 μg) and EDEM1-HA, EDEM2-HA, EDEM3-HA, or ER ManI-HA proteins (1 μg each). After 6 h, the culture medium was replaced with fresh or KIF-containing medium (100 μM). Forty-eight hours later, the cells were harvested and immunoprecipitated (*IP*) with anti-HA antibodies, after which Western blotting (*IB*) was performed with the indicated antibodies. Specific signals were quantified by densitometry, and the ratio between HCV E2 and HA (*right graph*) and between SEL1L and HA (*left graph*) in the same *lanes* is plotted on the graphs. The mean ± S.D. of three independent experiments are shown. *D*, EDEM protein-mediated ubiquitylation of HCV E2 protein in 293T cells in the absence or presence of KIF. The experimental procedure was the same as that described in Fig. 5*C*, except that immunoprecipitation was performed with anti-HCV E2 antibodies.

viruses is still unknown. To this end, we examined its role in the life cycle of JEV, another member of the Flaviviridae family. In contrast to HCV, KIF treatment had little effect on JEV production in infected cells (Fig. 6*A*) or the steady-state level of viral E glycoprotein (Fig. 6*B*). Interaction of EDEMs with JEV E was analyzed further. Neither EDEMs nor ER ManI was found to interact with JEV E in cells (Fig. 6*C*), indicating no significant role of the ERAD pathway in the JEV life cycle. Altogether, these results strongly suggest that the ERAD pathway is involved in the quality control of glycoproteins of specific viruses, possible through an interaction with EDEM(s), and subsequent regulation of virus production.

DISCUSSION

Accumulating evidence points to a role of the ERAD pathway in the pathogenesis of different genetic and degenerative diseases. However, the involvement of ERAD in the life cycle of viruses and infectious diseases remains poorly understood. Until recently, an experimental HCV cell culture infection system has been lacking such that studies evaluating the effect of HCV infection on the ERAD pathway were performed by either using HCV subgenomic replicons which lack structural proteins or by ectopic expression of one or multiple structural proteins (21, 22). However, this problem was solved by identifica-

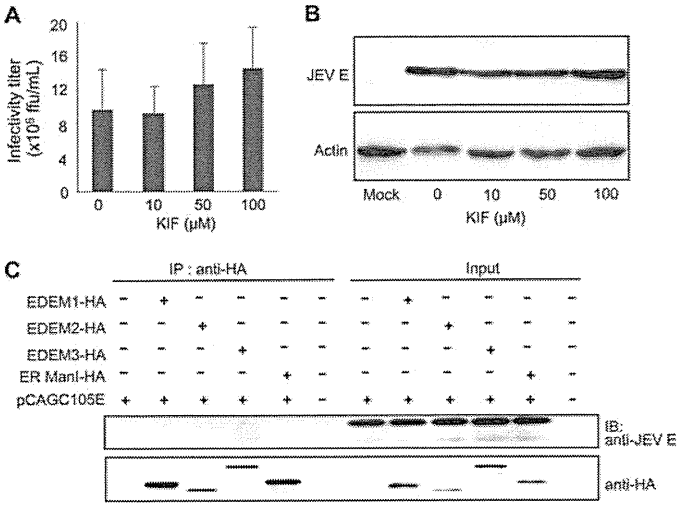

FIGURE 6. **Binding of JEV envelope glycoprotein with EDEMs and effect of KIF on JEV production.** *A*, JEV production in HuH-7 cells treated with KIF. The mean ± S.D. (*error bars*) of three independent experiments are shown. *B*, effect of KIF on the steady-state level of JEV envelope protein. *C*, binding of EDEMs with the JEV envelope.

tion of an HCV clone, JFH-1, capable of replicating and assembling infectious virus particles in cultured hepatocytes (15). In the present study, we used JFH-1 to examine the effect of HCV infection on activation of the ERAD pathway and its role in the virus life cycle. Our results show that the ERAD pathway is activated in HCV-infected cells, as evidenced by the maturation of XBP1 mRNA to its active form and up-regulation of EDEM1 (Fig. 1, *A–D*). Knocking down IRE1 reversed the induction of EDEM1, indicating that HCV infection-induced activation of the ERAD pathway is mediated through IRE1 (Fig. 1*F*). Loss- and gain-of-function analyses indicated that EDEM1 and EDEM3, particularly EDEM1, are involved in the post-translational control of HCV glycoproteins by which viral production is down-regulated (Figs. 3, *D* and *E*, and 4*A*). Our results suggest that EDEM1 and EDEM3 play a role in delivery of viral glycoproteins to the SEL1L-containing ubiquitin-ligase complex. It has recently been reported that coronavirus infection causes an accumulation of EDEM1 in membrane vesicles which are sites of viral replication, but that EDEM1 is not required for coronavirus replication (23). To our knowledge, the present study is the first to demonstrate regulation of the viral life cycle by ERAD machinery through interaction of EDEMs with viral glycoproteins.

We propose that the mechanisms described here are important during the early stages of establishing persistent HCV infection. ER stress caused by high levels of HCV infection during the acute phase presumably results in activation of the ERAD pathway. Induced EDEMs enhance the degradation of HCV envelope proteins, thereby reducing virus production. Maintenance of moderately low levels of HCV in the infected liver may contribute to the persistence of HCV infection, often associated with a lengthy asymptomatic phase that can last for decades. A range of viruses, including flaviviruses such as JEV, dengue virus, and West Nile virus, have been reported to induce XBP1 mRNA splicing triggered by ER stress (2, 3, 24). However, we demonstrate here that, in contrast to HCV, the envelope protein of JEV, which causes acute encephalitis, is not recognized by EDEMs, and the ERAD pathway does not control JEV production.

N-Linked glycoproteins displaying the glycan precursor Glc1Man9GlcNAc2 bind ER chaperones, such as calnexin or calreticulin, which facilitates protein folding. Removal of the terminal Glc from glycans disrupts this interaction with chaperones leading to Man trimming and delivery to ERAD machinery. A glucosyltransferase can transfer the terminal Man-linked Glc back to glycans, thereby allowing the "calnexin cycle" to continue until the glycoproteins are properly folded (for review, see Ref. 25). During this cycle, the decision of when to abandon additional folding attempts for immature polypeptides and to direct them instead toward the degradation pathway appears to be a crucial element of protein quality control. The basis by which this occurs, however, is not fully understood. Here, we demonstrate that stabilization of HCV envelope proteins and increased virus production occurs with KIF treatment (Fig. 5, *A* and *B*) and with gene silencing of either EDEM1 or EDEM3 (Figs. 3, *D* and *E*, and 4*A*). It is generally accepted that ERAD functions to eliminate proteins that are unable to adopt their native structure after translocation into the ER. From our results, however, one could argue that, during the HCV life cycle, at least a fraction of the competently folded viral glycoprotein intermediates may be released from the calnexin cycle before maturation and thereby be recognized as ERAD substrates. As suggested previously, the processes of protein folding and ERAD compete to some extent for newly synthesized polypeptides (26, 27). Under conditions in which high concentrations of ERAD-related factors are found in the ER due to induction of ER stress by viral infection, activated ERAD machinery may efficiently capture protein intermediates with folding/refolding capacity and cause premature termination of chaperone-assisted protein folding.

EDEM1 has recently been found to bind SEL1L, which is involved in the translocation of ERAD substrates from the ER to the cytoplasm (20). Our results demonstrate efficient binding of EDEM1 and EDEM3 to SEL1L, whereas EDEM2 exhibits only residual binding. In agreement with these results, increased ubiquitylation of HCV E2 protein was observed in cells overexpressing EDEM1 and EDEM3, but not in cells overexpressing the EDEM2 ortholog (Fig. 3*B*). Furthermore, KIF inhibited the binding of EDEM1 and EDEM3 with SEL1L, thus abrogating the ubiquitylation and enhancing the stability of HCV E2 protein (Fig. 5, *B* and *D*). It has been reported that KIF inhibits the interaction between EDEM1 and SEL1L, thus stabilizing ERAD substrates (4). Therefore, our results confirm previous findings and show that, along with EDEM1, KIF inhibits the binding of SEL1L to EDEM3. Furthermore, we have been the first to show that HCV E2 is a virus-derived ERAD substrate that can be used to analyze the mechanisms of this pathway. Taken together, our results indicate that EDEM1 and EDEM3, but not EDEM2, might be involved in targeting ERAD substrates to the translocation machinery, which may partly explain the different roles of the three EDEMs in HCV production. Although both EDEM1 and EDEM3 bind SEL1L and HCV envelope proteins, EDEM1 appears to have a larger role in regulation of HCV production than EDEM3. This is supported further by the finding that enhanced ubiquitylation of HCV E2 occurs in the presence

of EDEM1 overexpression (Figs. 3*B* and 5*D*). In EDEM3-knockdown cells, EDEM1 may take over the function of delivering ERAD substrates to the translocation machinery. We also speculate that EDEM1 may function as a helper for EDEM3. This is supported by the observation that EDEM1 and EDEM3 synergistically increase HCV production when knocked down together (data not shown). HCV glycoproteins are a suitable means by which to investigate differences and redundancies pertaining to the role of EDEMs in the ERAD pathway.

HCV-infected and TM-treated cells demonstrated the greatest activation of EDEM1 transcript production among EDEMs (Fig. 1, *C* and *D*, and supplemental Fig. S1). Although it is known that XBP1 binds to specific ER stress-responsive *cis*-acting elements to induce EDEMs (28, 29), the exact mechanism of transcriptional regulation is not fully understood. It will be interesting to examine regulatory mechanism(s) specific to individual EDEM homologs in an ER stress-dependent or -independent manner.

These findings highlight the crucial role of the ERAD pathway in the HCV life cycle. Further studies are needed to clarify the details of this complex pathway. The data generated in this work, however, further contribute to our understanding of the mechanisms that govern the maturation and fate of viral glycoproteins in the ER.

Acknowledgments—We thank Dr. F. V. Chisari for the HuH-7.5.1 cells, Drs. N. Hosokawa and K. Nagata for the EDEM expression plasmids, Dr. K. Mori for the reporter plasmids of GRP78 and GRP94, and Drs. C. K. Lim and T. Takasaki for the anti-JEV antibody. We thank Drs. Chia-Yi Yu and Yi-Ling Lin for valuable advice and T. Date, M. Kaga, M. Sasaki, and T. Mizoguchi for assistance.

REFERENCES

1. Vembar, S. S., and Brodsky, J. L. (2008) *Nat. Rev. Mol. Cell Biol.* **9,** 944–957
2. Yu, C. Y., Hsu, Y. W., Liao, C. L., and Lin, Y. L. (2006) *J. Virol.* **80,** 11868–11880
3. Barry, G., Fragkoudis, R., Ferguson, M. C., Lulla, A., Merits, A., Kohl, A., and Fazakerley, J. K. (2010) *J. Virol.* **84,** 7369–7377
4. Isler, J. A., Skalet, A. H., and Alwine, J. C. (2005) *J. Virol.* **79,** 6890–6899
5. Helenius, A., and Aebi, M. (2004) *Annu. Rev. Biochem.* **73,** 1019–1049
6. Mast, S. W., Diekman, K., Karaveg, K., Davis, A., Sifers, R. N., and Moremen, K. W. (2005) *Glycobiology* **15,** 421–436
7. Hirao, K., Natsuka, Y., Tamura, T., Wada, I., Morito, D., Natsuka, S., Romero, P., Sleno, B., Tremblay, L. O., Herscovics, A., Nagata, K., and Hosokawa, N. (2006) *J. Biol. Chem.* **281,** 9650–9658
8. Bartenschlager, R., and Lohmann, V. (2000) *J. Gen. Virol.* **81,** 1631–1648
9. Reed, K. E., and Rice, C. M. (2000) *Curr. Top. Microbiol. Immunol.* **242,** 55–84
10. Zhong, J., Gastaminza, P., Cheng, G., Kapadia, S., Kato, T., Burton, D. R., Wieland, S. F., Uprichard, S. L., Wakita, T., and Chisari, F. V. (2005) *Proc. Natl. Acad. Sci. U.S.A.* **102,** 9294–9299
11. Zhao, Z., Date, T., Li, Y., Kato, T., Miyamoto, M., Yasui, K., and Wakita, T. (2005) *J. Gen. Virol.* **86,** 2209–2220
12. Tani, H., Shiokawa, M., Kaname, Y., Kambara, H., Mori, Y., Abe, T., Moriishi, K., and Matsuura, Y. (2010) *J. Virol.* **84,** 2798–2807
13. Yoshida, H., Haze, K., Yanagi, H., Yura, T., and Mori, K. (1998) *J. Biol. Chem.* **273,** 33741–33749
14. Murakami, K., Kimura, T., Osaki, M., Ishii, K., Miyamura, T., Suzuki, T., Wakita, T., and Shoji, I. (2008) *J. Gen. Virol.* **89,** 1587–1592
15. Wakita, T., Pietschmann, T., Kato, T., Date, T., Miyamoto, M., Zhao, Z., Murthy, K., Habermann, A., Kräusslich, H. G., Mizokami, M., Bartenschlager, R., and Liang, T. J. (2005) *Nat. Med.* **11,** 791–796
16. Lim, C. K., Takasaki, T., Kotaki, A., and Kurane, I. (2008) *Virology* **374,** 60–70
17. Takeuchi, T., Katsume, A., Tanaka, T., Abe, A., Inoue, K., Tsukiyama-Kohara, K., Kawaguchi, R., Tanaka, S., and Kohara, M. (1999) *Gastroenterology* **116,** 636–642
18. Deng, L., Adachi, T., Kitayama, K., Bungyoku, Y., Kitazawa, S., Ishido, S., Shoji, I., and Hotta, H. (2008) *J. Virol. 82, 10375–10385*
19. Masaki, T., Suzuki, R., Saeed, M., Mori, K., Matsuda, M., Aizaki, H., Ishii, K., Maki, N., Miyamura, T., Matsuura, Y., Wakita, T., and Suzuki, T. (2010) *J. Virol. 84, 5824–5835*
20. Cormier, J. H., Tamura, T., Sunryd, J. C., and Hebert, D. N. (2009) *Mol. Cell* **34,** 627–633
21. Tardif, K. D., Mori, K., Kaufman, R. J., and Siddiqui, A. (2004) *J. Biol. Chem.* **279,** 17158–17164
22. Chan, S. W., and Egan, P. A. (2005) *FASEB J.* **19,** 1510–1512
23. Reggiori, F., Monastyrska, I., Verheije, M. H., Calì, T., Ulasli, M., Bianchi, S., Bernasconi, R., de Haan, C. A., and Molinari, M. (2010) *Cell Host Microbe* **7,** 500–508
24. Medigeshi, G. R., Lancaster, A. M., Hirsch, A. J., Briese, T., Lipkin, W. I., Defilippis, V., Früh, K., Mason, P. W., Nikolich-Zugich, J., and Nelson, J. A. (2007) *J. Virol.* **81,** 10849–10860
25. Molinari, M. (2007) *Nat. Chem. Biol.* **3,** 313–320
26. Eriksson, K. K., Vago, R., Calanca, V., Galli, C., Paganetti, P., and Molinari, M. (2004) *J. Biol. Chem.* **279,** 44600–44605
27. Wu, Y., Swulius, M. T., Moremen, K. W., and Sifers, R. N. (2003) *Proc. Natl. Acad. Sci. U.S.A.* **100,** 8229–8234
28. Olivari, S., Galli, C., Alanen, H., Ruddock, L., and Molinari, M. (2005) *J. Biol. Chem.* **280,** 2424–2428
29. Yoshida, H., Matsui, T., Hosokawa, N., Kaufman, R. J., Nagata, K., and Mori, K. (2003) *Dev. Cell* **4,** 265–271

In Vivo Adaptation of Hepatitis C Virus in Chimpanzees for Efficient Virus Production and Evasion of Apoptosis

Mohsan Saeed,[1,2] Masaaki Shiina,[3] Tomoko Date,[1] Daisuke Akazawa,[1] Noriyuki Watanabe,[1] Asako Murayama,[1] Tetsuro Suzuki,[1] Haruo Watanabe,[2,4] Nobuhiko Hiraga,[5] Michio Imamura,[5] Kazuaki Chayama,[5] Youkyung Choi,[6] Krzysztof Krawczynski,[6] T. Jake Liang,[7] Takaji Wakita,[1] and Takanobu Kato[1]

Hepatitis C virus (HCV) employs various strategies to establish persistent infection that can cause chronic liver disease. Our previous study showed that both the original patient serum from which the HCV JFH-1 strain was isolated and the cell culture–generated JFH-1 virus (JFH-1cc) established infection in chimpanzees, and that infected JFH-1 strains accumulated mutations after passage through chimpanzees. The aim of this study was to compare the *in vitro* characteristics of JFH-1 strains emerged in each chimpanzee at early and late stages of infection, as it could provide an insight into the phenomenon of viral persistence. We generated full-genome JFH-1 constructs with the mutations detected in patient serum-infected (JFH-1/S1 and S2) and JFH-1cc–infected (JFH-1/C) chimpanzees, and assessed their effect on replication, infectious virus production, and regulation of apoptosis in cell culture. The extracellular HCV core antigen secreted from JFH-1/S1-, S2-, and C-transfected HuH-7 cells was 2.5, 8.9, and 2.1 times higher than that from JFH-1 wild-type (JFH-1/wt) transfected cells, respectively. Single cycle virus production assay with a CD81-negative cell line revealed that the strain JFH-1/S2, isolated from the patient serum-infected chimpanzee at a later time point of infection, showed lower replication and higher capacity to assemble infectious virus particles. This strain also showed productive infection in human hepatocyte–transplanted mice. Furthermore, the cells harboring this strain displayed lower susceptibility to the apoptosis induced by tumor necrosis factor α or Fas ligand compared with the cells replicating JFH-1/wt. *Conclusion:* The ability of lower replication, higher virus production, and less susceptibility to cytokine-induced apoptosis may be important for prolonged infection *in vivo*. Such control of viral functions by specific mutations may be a key strategy for establishing persistent infection. (HEPATOLOGY 2011;00:000–000)

Currently, approximately 200 million people are infected with hepatitis C virus (HCV) and are at continuous risk of developing chronic liver diseases such as chronic hepatitis, liver cirrhosis, and hepatocellular carcinoma.[1,2] Although acute HCV infection elicits innate and adaptive immune responses, the virus successfully evades clearance in approximately 75% of infected individuals.[3,4] The mechanisms by

Abbreviations: Ag, antigen; CTL, cytotoxic T lymphocytes; FasL, Fas ligand; HCV, hepatitis C virus; JFH-1cc, cell culture–generated JFH-1 virus; JFH-1/wt, JFH-1 wild-type; MFI, mean fluorescence intensity; NK, natural killer, NS, nonstructural; PARP, poly(adenosine diphosphate ribose) polymerase; TNF-α, tumor necrosis factor α; TUNEL, terminal deoxynucleotidyl transferase–mediated deoxyuridine triphosphate nick-end labeling.

From the [1]Department of Virology II, National Institute of Infectious Diseases, Tokyo, Japan; the [2]Department of Infection and Pathology, Graduate School of Medicine, The University of Tokyo, Tokyo, Japan; the [3]Division of Gastroenterology, Tohoku University Graduate School of Medicine, Sendai, Japan; the [4]National Institute of Infectious Diseases, Tokyo, Japan; the [5]Department of Medicine and Molecular Science, Division of Frontier Medical Science, Programs for Biomedical Research, Graduate School of Biomedical Sciences, Hiroshima University, Hiroshima, Japan; the [6]Division of Viral Hepatitis, Center for Disease Control and Prevention, Atlanta, GA; and the [7]Liver Diseases Branch, National Institute of Diabetes and Digestive and Kidney Diseases, National Institutes of Health, Bethesda, MD.

Received November 26, 2010; accepted April 18, 2011.

Supported by grants-in-aid from the Japan Society for the Promotion of Science, the Ministry of Health, Labor, and Welfare of Japan, and the Ministry of Education, Culture, Sports, Science, and Technology, by the Research on Health Sciences Focusing on Drug Innovation from the Japan Health Sciences Foundation, and in part by the Intramural Research Program of the NIDDK, NIH (T. J. L.).

Tetsuro Suzuki is currently affiliated with the Department of Infectious Diseases, Hamamatsu University School of Medicine, Hamamatsu, Japan.

Address reprint requests to: Takanobu Kato, M.D., Ph.D., Department of Virology II, National Institute of Infectious Diseases, Tokyo, 162-8640, Japan. E-mail: takato@nih.go.jp; fax: (81)-3-5285-1161.

View this article online at wileyonlinelibrary.com.

DOI 10.1002/hep.24399

Potential conflict of interest: Nothing to report.

Additional Supporting Information may be found in the online version of this article.

which HCV leads to persistent infection at a high frequency are not yet fully understood. Lack of appropriate animal models, except chimpanzees, has rendered such studies difficult. Human hepatocyte-transplanted mice,[5,6] a useful small animal model to study HCV infection, are unsuitable to study the mechanisms of virus persistence because of a lack of B and T cell–mediated immunity.

HCV is a noncytopathic positive-stranded RNA virus of the *Flaviviridae* family. It primarily infects hepatocytes of humans and chimpanzees, where, thanks to error-prone RNA-dependent RNA polymerase, the infected virus accumulates a high number of mutations rapidly, thus providing opportunity for selection of viruses that have the ability to escape the immune system and establish persistent infection. Deciphering the strategies employed by HCV to establish persistence can be helpful in the development of new strategies to eradicate the virus and to stop disease progression. Until recently, the lack of an HCV strain having the ability to establish infection *in vivo* and *in vitro* was a substantial hindrance in studying the molecular mechanisms of virus persistence. This problem was solved by the identification of an HCV strain, JFH-1, that was isolated from a fulminant hepatitis patient and found to be capable of replicating and assembling infectious virus particles in chimpanzees as well as in cell culture.[7-10] This clone can be used to study the molecular mechanisms by which HCV evades the host immune system and causes chronic infection.

In a previous report, we inoculated patient serum from which the JFH-1 strain was originally isolated and cell culture–generated JFH-1 virus (JFH-1cc) into two different chimpanzees.[11] HCV established infection in both animals within 3 days of inoculation. In the JFH-1cc–infected chimpanzee, genome sequence of predominant infecting virus at week 2 was identical to JFH-1 wild-type (JFH-1/wt [in this study, this abbreviation was used instead of JFH-1 to distinguish it from other variant strains]), and the infecting virus has four synonymous and seven nonsynonymous mutations at week 7. In the JFH-1 patient serum–infected chimpanzee, 19 synonymous and six nonsynonymous mutations were observed in predominantly circulating virus at week 2, and this number increased to 35 synonymous and 17 nonsynonymous mutations at the later stage of infection course (week 23).[11] From these observations, we presumed that the isolates evolved in each chimpanzee at later stages of infection might have some advantage over the viruses isolated at earlier time points for survival in infected animals. Thus, in this study, we generated JFH-1 variants containing the mutations observed in these animals and assessed their effect on replication and infectious virus production in cell culture. Furthermore, we examined the effects of infection of these strains to tumor necrosis factor α (TNF-α)– or Fas ligand (FasL)–mediated apoptosis.

Materials and Methods

The complete Materials and Methods are provided in the Supporting Information.

Results

Effects of Mutations Identified in Chimpanzees. To investigate the effect of mutations on virus phenotype, we generated constructs containing the mutations observed in JFH-1 patient serum–infected chimpanzee and JFH-1cc–infected chimpanzee at various time points. The JFH-1 variants JFH-1/S1 and JFH-1/S2 contain the mutations observed in the patient serum–infected chimpanzee at week 2 and week 23, respectively, and JFH-1/C contains the mutations observed in the JFH-1cc–infected chimpanzee at week 7 (Supporting Table 1). The replication and virus production capacity of these variants in HuH-7 cells was compared with that of JFH-1/wt. After electroporation of *in vitro*–synthesized full-genome RNA of JFH-1/wt and variant strains, extracellular and intracellular HCV RNA and core antigen (Ag) were measured (Fig. 1). At day 5 posttransfection, all constructs displayed similar intracellular HCV RNA levels. However, extracellular HCV RNA level of JFH-1/C was 1.6 times higher than that of JFH-1/wt. Likewise, extracellular HCV RNA level of JFH-1/S2 was 3.4 times higher than that of JFH-1/S1 (Fig. 1A). Intracellular HCV core Ag levels of JFH-1/S2 and C were 240.9 $\pm$ 58.2 and 189.8 $\pm$ 42.1 fmol/mg protein, respectively, and were significantly lower ($P < 0.005$) than that of JFH-1/S1 (526.1 $\pm$ 58.2 fmol/mg protein) and JFH-1/wt (511.7 $\pm$ 32.9 fmol/mg protein) at day 1, but reached comparable levels at day 5 posttransfection. On the other hand, extracellular HCV core Ag level of JFH-1/C was 2.2 times higher than that of JFH-1/wt, and that of JFH-1/S2 was 3.6 times higher than that of JFH-1/S1 at day 5 posttransfection (Fig. 1B). Transfection efficiency of these strains, indicated by intracellular HCV core Ag levels at 4 hours posttransfection, was almost identical (data not shown).

Single Cycle Virus Production Assay. For detailed analysis of the effects of these mutations on different stages of the virus lifecycle, we used a Huh7-25 cell

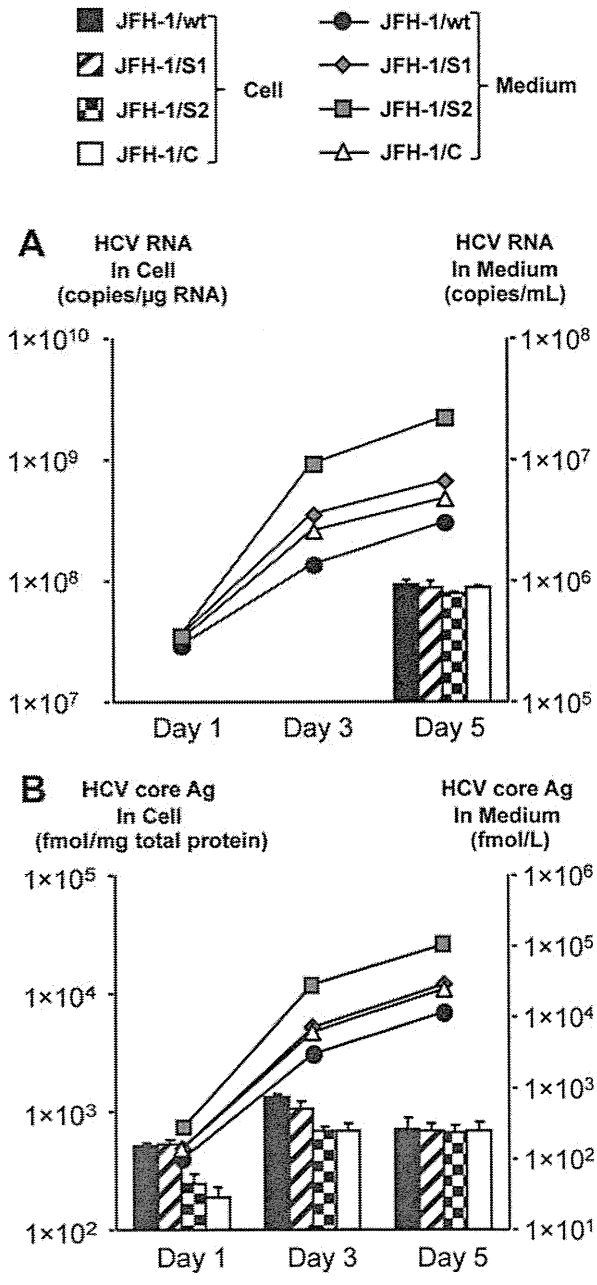

Fig. 1. Effects of *in vivo* adaptive mutations on virus production in HuH-7 cells. One million cells were transfected with 10 μg *in vitro*-transcribed RNA of JFH-1/wt, JFH-1/S1, JFH-1/S2, and JFH-1/C. (A) HCV RNA and (B) core Ag levels in cell lysates and medium were measured at the indicated time points. Assays were performed in triplicate, and data are presented as the mean ± SD.

line that lacks the surface expression of CD81, one of the cellular receptors for HCV entry. Three days after transfection with full-genome RNA of JFH-1/wt, JFH-1/S1, JFH-1/S2, and JFH-1/C, HCV RNA levels and infectivity titer were measured, and the specific infectivity was calculated (Table 1). Intracellular HCV RNA levels of JFH-1/C and JFH-1/S2 were lower than those of JFH-1/wt and S1, suggesting lower replication efficiency of these strains. However, the intracellular infectivity titers of JFH-1/C and JFH-1/S2 were 2.03 and 11.0 times higher than those of JFH-1/wt and JFH-1/S1, respectively ($P < 0.005$). Intracellular-specific infectivities (infectivity titer/HCV RNA copy number) of JFH-1/C and JFH-1/S2 showed more pronounced difference from those of JFH-1/wt and JFH-1/S1 (3.92 times and 12.9 times higher, respectively; $P < 0.005$). The infectious virus secretion rate (extracellular infectivity titer/intracellular infectivity titer) was not significantly different between JFH-1/wt and variant strains. These data indicate that mutations identified in chimpanzees at the later time point of infection led to reduced viral replication and increased assembly of infectious virus particles without any effect on viral release in cell culture.

Subgenomic Replicon Assay. To further confirm the replication efficiencies of strains observed in chimpanzees, we generated subgenomic replicons of JFH-1/wt, JFH-1/S1, JFH-1/S2, and JFH-1/C carrying the firefly luciferase reporter gene (SGR-JFH-1/Luc/wt, SGR-JFH-1/Luc/S1, SGR-JFH-1/Luc/S2, and SGR-JFH-1/Luc/C). *In vitro*–transcribed RNAs of these constructs were transfected into HuH-7 cells, and luciferase activity was measured to assess their replication capacity. The luciferase activities of SGR-JFH-1/Luc/C and SGR-JFH-1/Luc/S2 replicons were 7.30 and 7.33 times lower than those of SGR-JFH-1/Luc/wt and SGR-JFH-1/Luc/S1, respectively, at day 1 ($P < 0.00005$), suggesting attenuated replication capacities of variant replicons isolated from each animal at later time points of infection (Supporting Fig. 1A). The luciferase activity 4 hours after transfection was comparable, indicating similar levels of transfection efficiency (data not shown). Based on these data, we found that the mutations that emerged in nonstructural (NS)3-NS5B of JFH-1/S2 and JFH-1/C reduced the replication efficiency in cell culture.

Genomic Regions Responsible for Lower Replication and Higher Assembly of JFH-1/S2. To further clarify the genomic region responsible for lower replication efficiency and higher assembly rate of JFH-1/S2, we generated the chimeric constructs JFH-1/S2-wt and JFH-1/wt-S2 as described in the Supporting Materials and Methods. *In vitro*–transcribed RNAs of JFH-1/wt, JFH-1/S2, JFH-1/S2-wt, and JFH-1/wt-S2 were introduced into HuH-7 cells by electroporation and intracellular and extracellular HCV RNA and core Ag were measured. At day 5 posttransfection, all constructs displayed comparable intracellular HCV RNA levels (Fig. 2). However, extracellular HCV RNA levels of JFH-1/S2 and JFH-1/S2-wt were significantly

Table 1. Infectious Virus Production and Release of JFH-1/wt and Variants in Huh7-25 Cells

	Intracellular			Extracellular	Secretion Ratio (Extracellular/ Intracellular)
Strain	HCV RNA (copies/μg RNA)	Infectivity Titer (ffu/well)	Specific Infectivity (ffu/copies)	Infectivity Titer (ffu/well)	
JFH-1/wt	$7.75 \times 10^8 \pm 1.04 \times 10^8$	$4.21 \times 10^2 \pm 4.32 \times 10^1$	$2.09 \times 10^{-7} \pm 7.06 \times 10^{-8}$	$1.94 \times 10^3 \pm 3.76 \times 10^1$	4.6 ± 1.3
JFH-1/S1	$7.04 \times 10^8 \pm 8.49 \times 10^7$	$4.72 \times 10^2 \pm 5.63 \times 10^1$	$2.91 \times 10^{-7} \pm 6.00 \times 10^{-8}$	$3.02 \times 10^3 \pm 2.77 \times 10^2$	5.4 ± 2.0
JFH-1/S2	$4.16 \times 10^{8**} \pm 7.47 \times 10^6$	$5.19 \times 10^{3**} \pm 8.24 \times 10^1$	$3.76 \times 10^{-6**} \pm 7.01 \times 10^{-7}$	$3.23 \times 10^{4**} \pm 3.52 \times 10^3$	6.2 ± 3.0
JFH-1/C	$3.15 \times 10^{8*} \pm 5.02 \times 10^7$	$8.59 \times 10^{2*} \pm 4.81 \times 10^1$	$8.19 \times 10^{-7*} \pm 5.68 \times 10^{-8}$	$3.68 \times 10^3 \pm 3.02 \times 10^3$	4.3 ± 1.4
JFH-1/S2-wt	$7.07 \times 10^8 \pm 8.43 \times 10^7$	$4.40 \times 10^{3*} \pm 9.5 \times 10^1$	$2.73 \times 10^{-6*} \pm 2.35 \times 10^{-7}$	$3.0 \times 10^{4*} \pm 1.1 \times 10^3$	6.7 ± 0.7
JFH-1/wt-S2	$4.21 \times 10^{8*} \pm 1.97 \times 10^7$	$2.7 \times 10^2 \pm 2.9 \times 10^1$	$2.02 \times 10^{-7} \pm 4.0 \times 10^{-8}$	$1.7 \times 10^3 \pm 1.3 \times 10^2$	4.5 ± 0.4

Abbreviation: ffu, focus-forming units.
*$P < 0.005$ versus JFH-1/wt.
**$P < 0.005$ versus JFH-1/S1.

higher ($P < 0.0005$) than that of JFH-1/wt. On the other hand, extracellular RNA level of JFH-1/wt-S2 chimeric construct was lower than that of JFH-1/S2 and JFH-1/S2-wt and similar to that of JFH-1/wt. Likewise, extracellular core Ag levels of JFH-1/S2 and JFH-1/S2-wt were also significantly higher than that of JFH-1/wt. Intracellular HCV core Ag levels of JFH-1/S2 and JFH-1/wt-S2 on day 1 posttransfection were 240.9 ± 58.2 and 134.3 ± 17.1 fmol/mg protein, respectively, and were significantly lower ($P < 0.005$) than that of JFH-1/wt (526.1 ± 58.2 fmol/mg protein), whereas intracellular HCV core Ag level of JFH-1/S2-wt was comparable to that of JFH-1/wt. Transfection efficiency of these strains, indicated by intracellular HCV core Ag levels at 4 hours posttransfection, was almost identical (data not shown).

To further elucidate, we transfected Huh7-25 cells with *in vitro*–transcribed RNA of JFH-1/wt, JFH-1/S2, JFH-1/S2-wt, and JFH-1/wt-S2 and measured HCV RNA, core Ag, and infectivity titer in the cells and culture medium. Intracellular HCV RNA levels of JFH-1/S2 and JFH-1/wt-S2 were similar and lower than those of JFH-1/wt and JFH-1/S2-wt, suggesting mutations in NS3-NS5B were responsible for lower replication efficiency of JFH-1/S2 (Table 1). Intracellular infectivity titer of JFH-1/S2 and JFH-1/S2-wt was 12.3 and 10.4 times higher, respectively, than that of JFH-1/wt ($P < 0.005$) on day 3 posttransfection. The intracellular specific infectivities of JFH-1/S2 and JFH-1/S2-wt were significantly higher than that of JFH-1/wt (18 times and 13.1 times higher, respectively; $P < 0.005$). On the other hand, intracellular specific infectivity of JFH-1/wt-S2 was comparable to that of JFH-1/wt. The infectious virus secretion rate was not significantly different among all the constructs (Table 1). These data indicate that mutations emerged in the core-NS2 region of JFH-1/S2 are responsible for the enhanced assembly of infectious virus particles compared with JFH-1/wt.

Mapping Study for JFH-1/S2 Strain. Because our experiments with JFH-1/S2 subgenomic replicon and JFH-1/wt-S2 chimeric construct showed that mutations emerged in the NS3-NS5B region are responsible for reduced replication efficiency of JFH-1/S2, we performed mapping studies by generating various JFH-1 subgenomic replicons, each containing the mutations observed in individual nonstructural protein. Although mutations in NS4B and NS5A were associated with attenuated replication capacity of JFH-1, the most significant decrease in replication was observed with NS5B mutations (Supporting Fig. 1B).

For detailed analysis of mutations responsible for higher assembly, *in vitro*–transcribed RNAs of JFH-1/wt, JFH-1/S2, JFH-1/S2-wt, JFH-1/N397S, JFH-1/L752V, JFH-1/S2-NS2 (containing mutations G838R, A878V, and V881A), JFH-1/G838R, and JFH-1/A878V were transfected into Huh7-25 cells, and intracellular-specific infectivities were compared (Supporting Table 2). As reported previously, JFH1/G838R showed higher intracellular specific infectivity than that of JFH-1/wt, but could not reach the level of JFH-1/S2 or JFH-1/S2-wt. Among the mutants, intracellular specific infectivities of JFH1/L752V, JFH1/NS2, and JFH1/G838R were 4.02, 5.42, and 3.07 times higher than that of JFH-1/wt, but those of JFH1/N397S and JFH1/A878V were similar to that of JFH-1/wt. Thus, the combination of mutations in P7 and NS2 was found to contribute to the higher assembly of the JFH-1/S2 strain.

Human Hepatocyte–Transplanted Mouse Assay. To assess the *in vivo* infectivity of these strains, we inoculated culture medium containing 10^7 copies (HCV RNA titer measured by RTD-PCR) of JFH-1/wt, JFH-1/S1, JFH-1/S2, and C viruses into human

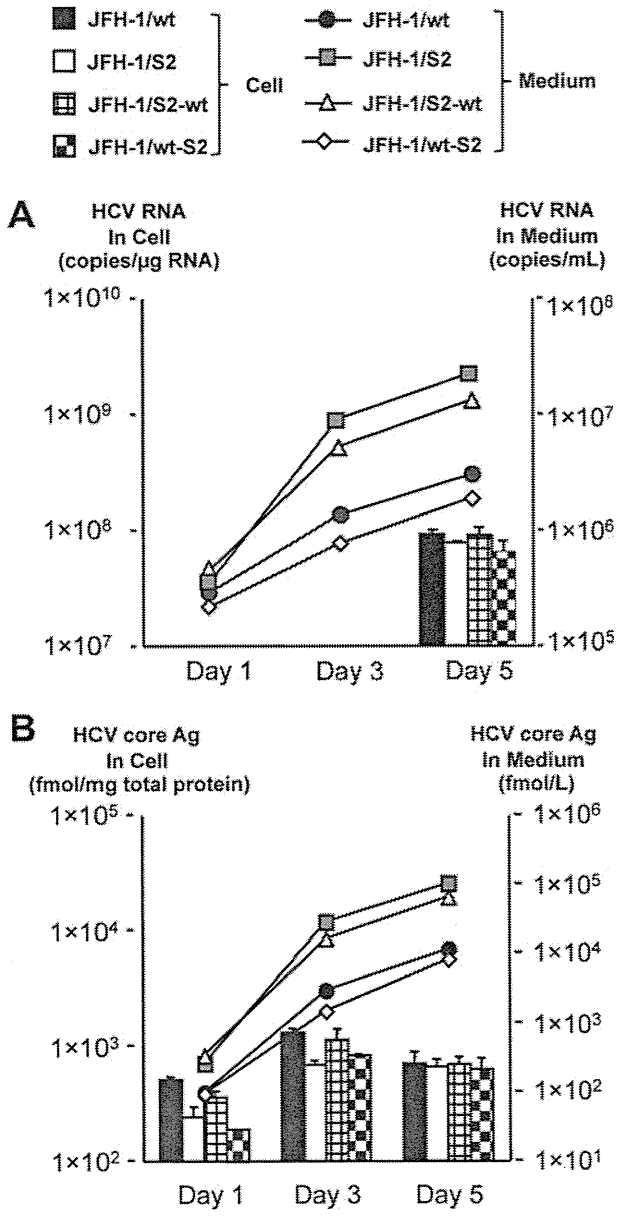

Fig. 2. Virus production of JFH-1/S2 chimeric constructs in HuH-7 cells. One million cells were transfected with 10 μg *in vitro*-transcribed RNA of JFH-1/wt, JFH-1/S2, JFH-1/S2-wt, and JFH-1/wt-S2. (A) HCV RNA and (B) core Ag levels in cell lysates and medium were measured at the indicated time points. Assays were performed in triplicate, and data are presented as the mean ± SD.

hepatocyte-transplanted mice. Two mice were used for each virus. Two weeks after intravascular inoculation, all mice but one became HCV RNA–positive (Fig. 3). Two mice died 3 weeks after inoculation; one was inoculated with JFH-1/wt and had developed infection, and the other was inoculated with JFH-1/C and died without developing infection. HCV RNA levels in infected mice fluctuated, ranging from 10^6 to 10^9 copies/mL. We could not observe much difference of infected HCV RNA titer among these inoculated mice. Sequence analyses of the complete open reading frames revealed that infecting JFH-1/wt virus and variant strains had no nonsynonymous mutations at the time of development of infection. From these data, we concluded that not only JFH-1/wt virus but also JFH-1/S1, JFH-1/S2, and JFH-1/C viruses were able to establish productive infection in human hepatocyte-transplanted mice.

Apoptosis Induction Assay. To investigate the survival strategy against the host defense system, we examined the susceptibility of JFH-1/wt and variant strains to TNF-α–mediated apoptosis induction. After transfection with *in vitro*–transcribed RNA of JFH-1/wt, JFH-1/S1, JFH-1/S2, and JFH-1/C, Huh-7.5.1 cells were exposed to TNF-α plus actinomycin D. Without exposure, apoptosis was observed in a limited number of HCV-positive cells (Supporting Fig. 2A). Forty-eight hours later, cells were harvested, fixed, and

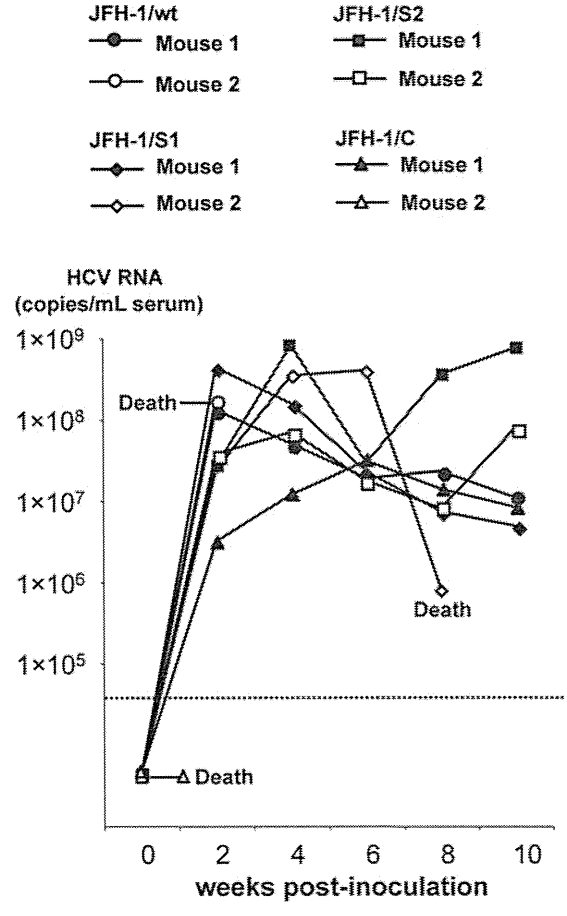

Fig. 3. *In vivo* infection study of JFH-1/wt and its variants in human hepatocyte-transplanted mice. Cell culture medium containing 1×10^7 HCV RNA copies of JFH-1/wt, JFH-1/S1, JFH-1/S2, and JFH-1/C were inoculated into human hepatocyte-transplanted mice, and HCV RNA levels in mice serum were monitored.

subjected to terminal deoxynucleotidyl transferase–mediated deoxyuridine triphosphate nick-end labeling (TUNEL) assay and anti-HCV NS5A staining. The effects of JFH-1/wt, JFH-1/S1, JFH-1/S2, and JFH-1/C transfection on apoptosis induction were determined by calculating the ratio of apoptosis between HCV-positive and HCV-negative populations and expressed as an apoptosis induction index. After treatment of JFH-1/wt–transfected cells with TNF-α, apoptosis was observed in 36.8% of the HCV-positive population and in 19.3% of the HCV-negative population, and the apoptosis induction index was 1.85 ± 0.06 (Fig. 4). The apoptosis induction indexes of JFH-1/S1–transfected and JFH-1/C– transfected cells were 1.23 ± 0.06 and 1.16 ± 0.10, respectively, suggesting lower susceptibility to apoptosis induction compared with JFH-1/wt. On the other hand, the apoptosis induction index of JFH-1/S2 was 0.74 ± 0.17, which was substantially lower than that of JFH-1/wt, demonstrating the more reduced apoptosis in the cells harboring this strain. Similar results were obtained by treatment with FasL plus actinomycin D (Supporting Fig. 2B). To confirm the lower susceptibility of JFH-1/S2–transfected cells, apoptosis was also detected by staining with anticleaved poly(adenosine diphosphate ribose) polymerase (PARP) antibody. The apoptosis induction indexes of JFH-1/wt and JFH-1/S2–transfected cells were 2.28 ± 0.24 and 1.15 ± 0.14, respectively, and were consistent with TUNEL assay (Fig. 5). Although the HCV NS5A-positive rate in JFH-1/S2–transfected cells was higher than that in JFH-1/wt, the mean fluorescence intensity of the NS5A-positive population in JFH-1/S2–transfected cells was significantly lower (185.0 ± 8.7) than that in JFH-1/wt–transfected cells (395.0 ± 98.0), corresponding to the observed phenotype of the JFH-1/S2 strain in the single cycle virus production assay (i.e., lower replication efficiency and rapid spread to surrounding cells).

To clarify the genomic region responsible for lower susceptibility of JFH-1/S2 to cytokine-induced apoptosis, we examined the effect of TNF-α on the cells carrying subgenomic reporter replicons. The apoptosis induction index of SGR-JFH1/Luc/S2–transfected cells was lower than that of SGR-JFH1/Luc/wt–transfected cells (Supporting Fig. 2C); however, the difference was not as pronounced as with full-genome constructs, indicating that mutations in the NS3-NS5B region contribute to lower susceptibility of JFH-1/S2 to cytokine-induced apoptosis, but they are not sufficient to explain the difference between JFH-1/wt and JFH-1/S2. We confirmed these results by use of the chimeric

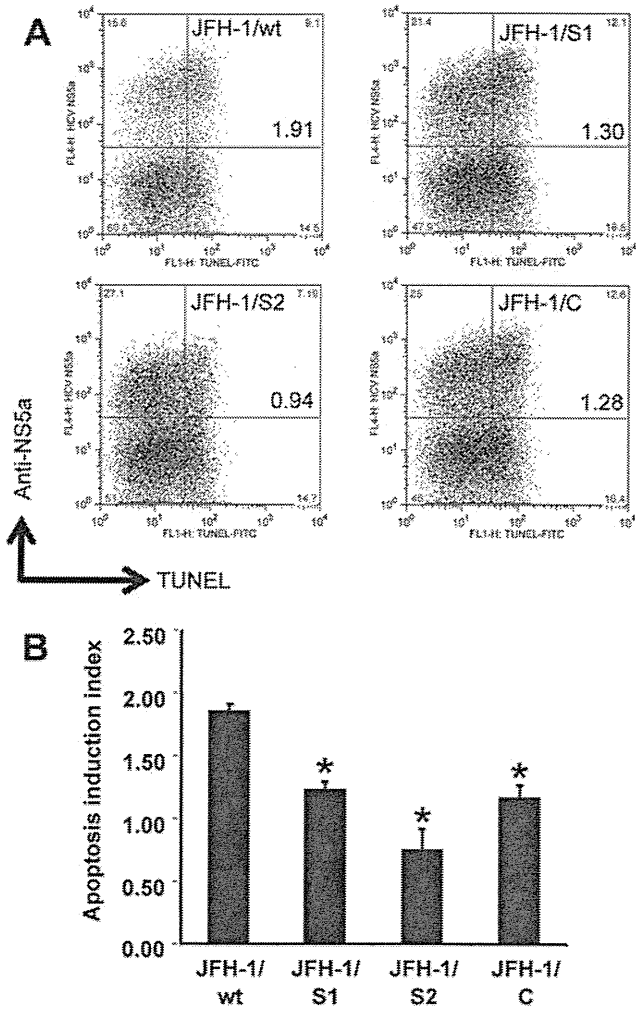

Fig. 4. Apoptosis induction in Huh-7.5.1 cells transfected with JFH-1/wt and its variants. (A) Three million cells were transfected with 3 μg *in vitro*-transcribed full-genome RNA of JFH-1/wt, JFH-1/S1, JFH-1/S2, and JFH-1/C. Forty-eight hours later, apoptosis was induced by exposing cells to 20 ng/mL TNF-α plus 50 ng/mL actinomycin D. Cells were harvested after 48 hours of treatment and subjected to TUNEL and anti-HCV NS5A staining. Dot plots show HCV replication and apoptosis at the single cell level. Quadrant gates were determined using unstained and a terminal deoxynucleotidyltrasferase-untreated control in each culture condition. The clone names and apoptosis induction indexes are indicated in the upper right box. (B) Apoptosis induction indexes of JFH-1/wt-, JFH-1/S1-, JFH-1/S2-, and JFH-1/C- transfected cells. The mean ± SD of three independent experiments is shown. *$P < 0.005$ versus JFH-1/wt.

constructs JFH-1/S2-wt and JFH-1/wt-S2. The apoptosis induction indexes of JFH-1/S2-wt–transfected and JFH-1/wt-S2–transfected cells were 1.42 ± 0.13 and 1.71 ± 0.08, respectively (Fig. 5). These data indicate that both structural and nonstructural regions of JFH-1/S2 were associated with lower susceptibility to cytokine-induced apoptosis, although mutations in core-NS2 seemed to have higher contribution toward this phenotype. Together, these results indicate that the JFH-1/S2 strain, which was selected after passage in

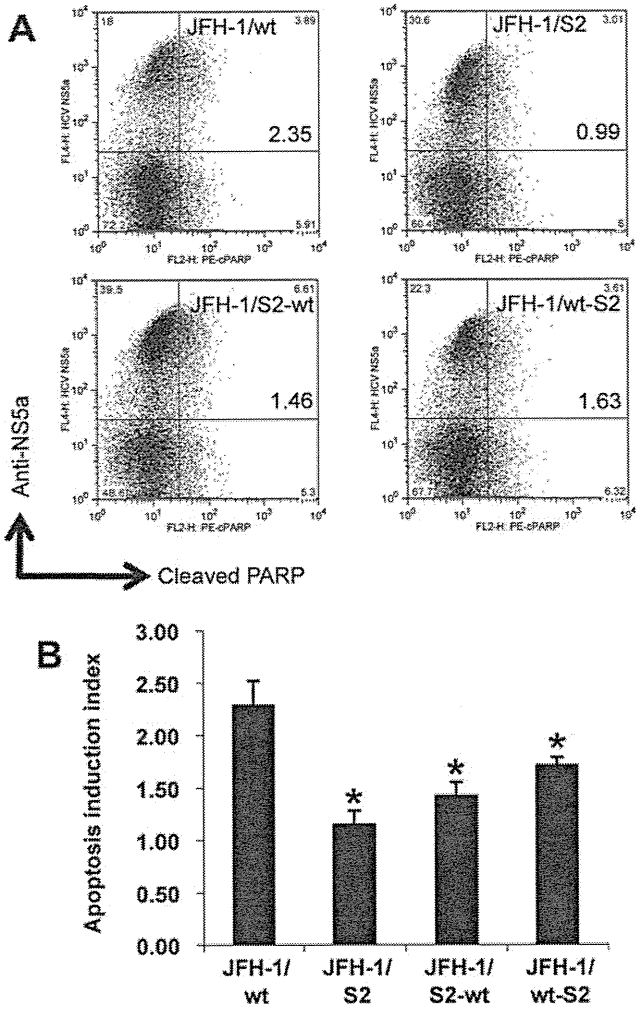

Fig. 5. Apoptosis induction in Huh-7.5.1 cells transfected with JFH-1/wt, JFH-1/S2, and their chimeric constructs. (A) Three million cells were transfected with 3 μg *in vitro*-transcribed full-genome RNA of JFH-1/wt, JFH-1/S2, JFH-1/S2-wt, and JFH-1/wt-S2. Apoptosis was induced by exposing cells to 20 ng/mL TNF-α plus 50 ng/mL actinomycin D and detected by anticleaved PARP staining. The clone names and apoptosis induction indexes are indicated in the upper right box. (B) Apoptosis induction indexes of JFH-1/wt-, JFH-1/S2-, JFH-1/S2-wt-, and JFH-1/wt-S2-transfected cells. The mean ± SD of three independent experiments is shown. *$P < 0.05$ versus JFH-1/wt.

the patient serum–infected chimpanzee, acquired less susceptibility to the cytokine-induced apoptosis.

Discussion

HCV develops chronic infection in the vast majority of infected patients[1]; however, the mechanisms of its persistence are still under investigation. Many viruses have evolved different strategies to cope with host immune systems, thus causing the development of persistent infection. For example, some viruses interfere with the major histocompatibility complex class I presentation of viral antigens, whereas others modulate lymphocyte and macrophage functions, including cytokine production.[12-16] In our previous study, we detected an increasing number of mutations in the HCV genome isolated from JFH-1 patient serum–infected chimpanzees. Thus, we reasoned that these detected mutations might have imparted some advantage to this virus for long-time survival. To examine this hypothesis, we compared the phenotypes of JFH-1 variant strains emerged at early and late stages of infection in JFH-1 patient serum–infected and JFH-1cc–infected chimpanzees and found that the JFH-1/S2 strain isolated from the patient serum–infected chimpanzee at a later time point of infection replicated slowly, produced more infectious viruses, and displayed reduced susceptibility to cytokine-induced apoptosis.

The JFH-1 variant strain JFH-1/C, which contains seven nonsynonymous mutations identified in the JFH-1cc–infected chimpanzee at week 7, showed comparatively slower replication kinetics and slightly enhanced infectious virus production in cell culture. The intracellular specific infectivity of this strain in Huh7-25 cells was 3.9 times higher than that of JFH-1/wt (Table 1). These characteristics might have imparted some advantage to this strain for establishing productive infection in the chimpanzee. The other JFH-1 variant strains, JFH-1/S1 and JFH-1/S2, contain 6 and 17 nonsynonymous mutations identified in the JFH-1 patient serum–infected chimpanzee at weeks 2 and 23 postinfection, respectively. Replication kinetics and infectious virus production of the JFH-1/S1 strain were comparable to that of JFH-1/wt in cultured cells (Fig. 1, Table 1). In contrast, the JFH-1/S2 strain showed lower replication efficiency. Although the intracellular HCV RNA level of this strain in Huh7-25 cells was lower than that of JFH-1/wt and JFH-1/S1, and almost the same as that of JFH-1/C (Table 1), intracellular specific infectivity was 18.0 and 12.9 times higher than that of JFH-1/wt and JFH-1/S1, respectively, suggesting a significant increase in the assembly of infectious virus particles ($P < 0.005$, Table 1). The enhanced capacity of this strain to assemble infectious virus particles resulted in a higher extracellular infectivity titer that contributed to the rapid spread of virus to surrounding cells. Flow cytometry analyses of cells transfected with JFH-1/wt and variant strains revealed that the percentage of the HCV NS5A-positive population in JFH-1/S2–transfected cells was higher, but the mean fluorescence intensity of the anti-NS5A signal was lower than that in JFH-1/wt–transfected cells, thus confirming higher spread and lower replication of this strain. Taken together, both JFH-1/C and JFH-1/S2 exhibited a tendency toward

decreased replication and increased infectious virus production. However, the extent of enhanced virus production was substantially lower in JFH-1/C than in JFH-1/S2, which might have led to the earlier elimination of infection in the JFH-1cc–infected chimpanzee. In other words, the potency of infectious virus production and spread seems to correspond to the duration of infection in infected animals.

The association between a lower replication efficiency and persistent infection is still unclear. It has been reported that an escape mutant with an amino acid substitution at the cytotoxic T lymphocyte (CTL) epitope in the NS3 region exhibits lower NS3/4 protease activity and replication capacity *in vitro*.[17,18] The JFH-1/S2 strain contains the T1077A mutation in the NS3 region (Supporting Table 1), and this mutation is located close to mutations reported to be associated with immune evasion and lower replication.[17] Thus, the lower replication efficiency of the JFH-1/S2 strain may be a result of an immune escape mutation at the expense of viral fitness. Meanwhile, we cannot deny the advantage of lower replication in establishing persistent infection. Lower replication may contribute to the avoidance of major histocompatibility class I–mediated antigen presentation and to escape from the host immune system. Either way, by acquiring the ability to produce more viral particles, the JFH-1/S2 strain could rapidly spread to surrounding cells, irrespective of its lower replication efficiency. Importantly, these emerged mutations did not attenuate *in vivo* infectivity, unlike cell culture adaptive mutations reported to cause attenuated infection *in vivo*.[19] Upon inoculation into human hepatocyte–transplanted mice, JFH-1/S1, JFH-1/S2, and JFH-1/C strains could establish infection without any mutations, produced levels of viremia similar to JFH-1/wt, and persisted for a similar observed period of infection (Fig. 2). This observation is different from that in chimpanzees, where JFH-1/wt and JFH-1/C strains were eliminated earlier than JFH-1/S2. In contrast to chimpanzees, human hepatocyte–transplanted mice lack a CTL and natural killer (NK) cell–mediated immune system, which could be responsible for this difference.[6] Taken together, our results suggest that along with efficient infectious virus production, the JFH-1/S2 strain might have acquired an advantage that helps it evade the CTL and NK cell–mediated immune system.

Apoptosis of virus-infected cells by the immune system is crucial as a general mechanism of clearing infections.[20,21] The J6/JFH-1 chimeric virus has been reported to exhibit proapoptotic characteristics in cell culture.[22] However, because HCV needs to escape the host immune system in order to establish chronic infection, immune cell–mediated apoptosis may be inhibited in infected hepatocytes. In the liver, HCV-infected hepatocytes are eliminated by targeted apoptosis induced by NK cells, macrophages, and CTLs with ligand-mediated and receptor-mediated signals such as TNF-α, FasL, and TNF-related apoptosis–inducing ligand.[23-26] Thus, we used TNF-α to mimic natural immunomediated apoptosis and found that the JFH-1/S2–replicating cells have lower susceptibility to the apoptosis induced by these cytokines. In JFH-1/S2–transfected cells, TNF-α–induced apoptosis detected by TUNEL assay was substantially lower than that of JFH-1/wt–transfected cells (Fig. 4). We confirmed it by staining with anticleaved PARP. In complete agreement with the results produced by way of TUNEL assay, the number of anticleaved PARP stained cells among JFH-1/S2–infected cells was significantly lower than that among JFH-1/wt–infected cells (Fig. 5). In our previous study, we reported that HCV-specific immune responses with T cell proliferation and interferon-γ production were maintained until the disappearance of viremia in the patient serum–infected chimpanzee.[11] This finding indicates that continuous selection pressure in the infected chimpanzee might have contributed to the emergence of a clone with an ability to escape the cytokine-induced apoptosis. We are not sure whether this phenotype of JFH-1/S2 is due to its lower replication efficiency and thus lower production of HCV proteins. The accumulation of viral proteins might predispose cells to the apoptosis induced by TNF-α. To answer this question, it will be necessary to investigate the genomic regions of JFH-1/S2 and cellular host factors responsible for the ability of this strain to escape the apoptosis.

By way of mapping analysis for JFH-1/S2, we could determine responsible regions; NS5B was for lower replication efficiency (Supporting Fig. 1B), and P7 and NS2 were for enhanced viral particle assembly (Supporting Table 2). For the evasion of apoptosis, we could not specify the responsible region, because both chimeric constructs, JFH-1/S2-wt and JFH-1/wt-S2, showed less susceptibility to cytokine-induced apoptosis to a certain extent. These data indicate that both structural and nonstructural regions might have contributed to the acquisition of this phenotype. Previously, a potent antiapoptotic effect of the HCV NS5A protein was described.[27] NS5A interacts with Bin1, which is a nucleocytoplasmic c-Myc–interacting protein with tumor suppressor and apoptotic properties, thus inhibiting Bin1-

associated apoptosis. Because JFH-1/S2 contains several mutations in the NS5A region (Supporting Table 1), one or more mutations in this protein may be associated with antiapoptotic effects.

In conclusion, we demonstrated that the JHF-1/S2 strain acquired phenotypes of lower replication, higher virus production, and less susceptibility to cytokine-induced apoptosis. These phenotypes were associated with mutations that emerged 23 weeks after infection in a chimpanzee, and might have contributed to long-term infection *in vivo*. Such control of viral functions by specific mutations may be a key viral strategy to establish persistent infection.

Acknowledgment: We are grateful to Francis V. Chisari for providing the Huh-7.5.1 cell line and Nao Sugiyama for technical assistance.

References

1. Liang TJ, Rehermann B, Seeff LB, Hoofnagle JH. Pathogenesis, natural history, treatment, and prevention of hepatitis C. Ann Intern Med 2000;132:296-305.
2. Feld JJ, Liang TJ. Hepatitis C—identifying patients with progressive liver injury. HEPATOLOGY 2006;43:S194-S206.
3. Thimme R, Oldach D, Chang KM, Steiger C, Ray SC, Chisari FV. Determinants of viral clearance and persistence during acute hepatitis C virus infection. J Exp Med 2001;194:1395-1406.
4. Thimme R, Bukh J, Spangenberg HC, Wieland S, Pemberton J, Steiger C, et al. Viral and immunological determinants of hepatitis C virus clearance, persistence, and disease. Proc Natl Acad Sci U S A 2002;99:15661-15668.
5. Mercer DF, Schiller DE, Elliott JF, Douglas DN, Hao C, Rinfret A, et al. Hepatitis C virus replication in mice with chimeric human livers. Nat Med 2001;7:927-933.
6. Tateno C, Yoshizane Y, Saito N, Kataoka M, Utoh R, Yamasaki C, et al. Near completely humanized liver in mice shows human-type metabolic responses to drugs. Am J Pathol 2004;165:901-912.
7. Kato T, Furusaka A, Miyamoto M, Date T, Yasui K, Hiramoto J, et al. Sequence analysis of hepatitis C virus isolated from a fulminant hepatitis patient. J Med Virol 2001;64:334-339.
8. Wakita T, Pietschmann T, Kato T, Date T, Miyamoto M, Zhao Z, et al. Production of infectious hepatitis C virus in tissue culture from a cloned viral genome. Nat Med 2005;11:791-796.
9. Zhong J, Gastaminza P, Cheng G, Kapadia S, Kato T, Burton DR, et al. Robust hepatitis C virus infection in vitro. Proc Natl Acad Sci U S A 2005;102:9294-9299.
10. Lindenbach BD, Evans MJ, Syder AJ, Wolk B, Tellinghuisen TL, Liu CC, et al. Complete replication of hepatitis C virus in cell culture. Science 2005;309:623-626.
11. Kato T, Choi Y, Elmowalid G, Sapp RK, Barth H, Furusaka A, et al. Hepatitis C virus JFH-1 strain infection in chimpanzees is associated with low pathogenicity and emergence of an adaptive mutation. HEPATOLOGY 2008;48:732-740.
12. Johannessen I, Crawford DH. In vivo models for Epstein-Barr virus (EBV)-associated B cell lymphoproliferative disease (BLPD). Rev Med Virol 1999;9:263-277.
13. Oglesbee MJ, Pratt M, Carsillo T. Role for heat shock proteins in the immune response to measles virus infection. Viral Immunol 2002;15:399-416.
14. Stevenson PG, Boname JM, de Lima B, Efstathiou S. A battle for survival: immune control and immune evasion in murine gamma-herpesvirus-68 infection. Microbes Infect 2002;4:1177-1182.
15. Alcami A. Viral mimicry of cytokines, chemokines and their receptors. Nat Rev Immunol 2003;3:36-50.
16. Wilkinson GW, Tomasec P, Stanton RJ, Armstrong M, Prod'homme V, Aicheler R, et al. Modulation of natural killer cells by human cytomegalovirus. J Clin Virol 2008;41:206-212.
17. Soderholm J, Ahlen G, Kaul A, Frelin L, Alheim M, Barnfield C, et al. Relation between viral fitness and immune escape within the hepatitis C virus protease. Gut 2006;55:266-274.
18. Uebelhoer L, Han JH, Callendret B, Mateu G, Shoukry NH, Hanson HL, et al. Stable cytotoxic T cell escape mutation in hepatitis C virus is linked to maintenance of viral fitness. PLoS Pathog 2008;4:e1000143.
19. Bukh J, Pietschmann T, Lohmann V, Krieger N, Faulk K, Engle RE, et al. Mutations that permit efficient replication of hepatitis C virus RNA in Huh-7 cells prevent productive replication in chimpanzees. Proc Natl Acad Sci U S A 2002;99:14416-14421.
20. Kagi D, Seiler P, Pavlovic J, Ledermann B, Burki K, Zinkernagel RM, et al. The roles of perforin- and Fas-dependent cytotoxicity in protection against cytopathic and noncytopathic viruses. Eur J Immunol 1995;25:3256-3262.
21. Kagi D, Vignaux F, Ledermann B, Burki K, Depraetere V, Nagata S, et al. Fas and perforin pathways as major mechanisms of T cell-mediated cytotoxicity. Science 1994;265:528-530.
22. Deng L, Adachi T, Kitayama K, Bungyoku Y, Kitazawa S, Ishido S, et al. Hepatitis C virus infection induces apoptosis through a Bax-triggered, mitochondrion-mediated, caspase 3-dependent pathway. J Virol 2008;82:10375-10385.
23. Kafrouni MI, Brown GR, Thiele DL. Virally infected hepatocytes are resistant to perforin-dependent CTL effector mechanisms. J Immunol 2001;167:1566-1574.
24. Guicciardi ME, Gores GJ. Apoptosis: a mechanism of acute and chronic liver injury. Gut 2005;54:1024-1033.
25. Fischer R, Baumert T, Blum HE. Hepatitis C virus infection and apoptosis. World J Gastroenterol 2007;13:4865-4872.
26. Stegmann KA, Bjorkstrom NK, Veber H, Ciesek S, Riese P, Wiegand J, et al. Interferon-alpha-induced TRAIL on natural killer cells is associated with control of hepatitis C virus infection. Gastroenterology 2010;138:1885-1897.
27. Nanda SK, Herion D, Liang TJ. The SH3 binding motif of HCV NS5A protein interacts with Bin1 and is important for apoptosis and infectivity. Gastroenterology 2006;130:794-809.

Biochemical and Biophysical Research Communications 410 (2011) 404–409

Contents lists available at ScienceDirect

Biochemical and Biophysical Research Communications

journal homepage: www.elsevier.com/locate/ybbrc

Development of recombinant hepatitis C virus with NS5A from strains of genotypes 1 and 2

Yuka Okamoto [a,b], Takahiro Masaki [a], Asako Murayama [a], Tsubasa Munakata [c], Akio Nomoto [d], Shingo Nakamoto [e], Osamu Yokosuka [e], Haruo Watanabe [b,f], Takaji Wakita [a], Takanobu Kato [a,*]

[a] Department of Virology II, National Institute of Infectious Diseases, Shinjuku-ku, Tokyo 162-8640, Japan
[b] Department of Pathology, Immunology, and Microbiology, Graduate School of Medicine, The University of Tokyo, Bunkyo-ku, Tokyo 113-0033, Japan
[c] The Tokyo Metropolitan Institute of Medical Science, Setagaya-ku, Tokyo 156-8506, Japan
[d] Institute of Microbial Chemistry, Shinagawa-ku, Tokyo 141-0021, Japan
[e] Department of Medicine and Clinical Oncology, Graduate School of Medicine, Chiba University, Chiba 260-0856, Japan
[f] National Institute of Infectious Diseases, Shinjuku-ku, Tokyo 162-8640, Japan

ARTICLE INFO

Article history:
Received 26 May 2011
Available online 6 June 2011

Keywords:
HCV
NS5A inhibitor
Virus assembly
JFH-1

ABSTRACT

Nonstructural protein 5A (NS5A) of hepatitis C virus (HCV) plays multiple and diverse roles in the viral lifecycle, and is currently recognized as a novel target for anti-viral therapy. To establish an HCV cell culture system with NS5A of various strains, recombinant viruses were generated by replacing NS5A of strain JFH-1 with those of strains of genotypes 1 (H77; 1a and Con1; 1b) and 2 (J6CF; 2a and MA; 2b). All these recombinant viruses were capable of replication and infectious virus production. The replacement of JFH-1 NS5A with those of genotype 1 strains resulted in similar or slightly reduced virus production, whereas replacement with those of genotype 2 strains enhanced virus production as compared with JFH-1 wild-type. A single cycle virus production assay with a CD81-negative cell line revealed that the efficient virus production elicited by replacement with genotype 2 strains depended on enhanced viral assembly, and that substitutions in the C-terminus of NS5A were responsible for this phenotype. Pulse-chase assays revealed that these substitutions in the C-terminus of NS5A were possibly associated with accelerated cleavage kinetics at the NS5A–NS5B site. Using this cell culture system with NS5A-substituted recombinant viruses, the anti-viral effects of an NS5A inhibitor were then examined. A 300- to 1000-fold difference in susceptibility to the inhibitor was found between strains of genotypes 1 and 2. This system will facilitate not only a better understanding of strain-specific roles of NS5A in the HCV lifecycle, but also enable the evaluation of genotype and strain dependency of NS5A inhibitors.

1. Introduction

Approximately 3% of the world's population is persistently infected with hepatitis C virus (HCV) and at increased risk of fatal chronic liver diseases such as decompensated liver cirrhosis and hepatocellular carcinoma. HCV have significant diversity in their genome and are grouped into six major genotypes. Among these genotypes, genotypes 1 and 2 are distributed worldwide and are predominant in Japan. The genotype is an important viral factor to predict the outcome of interferon (IFN)-based therapy. Because the efficacy of current therapy with pegylated IFN and ribavirin is insufficient, there is great interest in the development of novel HCV-specific inhibitors. The development of an HCV cell culture system with strain JFH-1 has enabled the study of the viral lifecycle and research into anti-viral compounds [1]. However, the available strains used in the HCV cell culture system are still limited to JFH-1 (genotype 2a) and H77S (genotype 1a) [2]. Thus, JFH-1 based recombinant viruses harboring specific regions of other strains would be useful to assess the genotype or strain-specific sensitivity to novel anti-HCV compounds.

Although NS5A is an essential and involved in HCV RNA replication and virus assembly [3,4], it has been reported to be tolerable for trans-complementation in replication-defective mutants due to critical mutations in NS5A [5]. We hypothesized that the NS5A of strain JFH-1 could be replaced with those of other strains. In the present study, we developed a cell culture system with JFH-1 based intra- and inter-genotypic recombinant HCV harboring NS5A of strains H77 (genotype 1a) [6], Con1 (genotype 1b) [7], J6CF (genotype 2a) [8], and MA (genotype 2b) [9]. Through the use of these recombinant viruses, we evaluated the effects of NS5A replacement on the HCV lifecycle and susceptibility to the NS5A inhibitor BMS-790052.

* Corresponding author. Address: Department of Virology II, National Institute of Infectious Diseases, 1-23-1 Toyama, Shinjuku-ku, Tokyo 162-8640, Japan. Fax: +81 3 5285 1161.
E-mail address: takato@nih.go.jp (T. Kato).

0006-291X/$ - see front matter © 2011 Elsevier Inc. All rights reserved.
doi:10.1016/j.bbrc.2011.05.144

2. Materials and methods

2.1. Cell culture

The human hepatoma cell line, HuH-7, and derivative cell lines, Huh7.5.1 [10] and Huh7-25 [11], were cultured in complete growth medium as described previously [1,11].

2.2. Plasmid construction

Plasmids containing the full-genome of HCV strain JFH-1 (pJFH1) and of a replication defective mutant (pJFH1/GND) have been described previously [1]. The construction of the NS5A replaced recombinant viruses and subgenomic reporter replicons was described in Supplementary materials.

2.3. In vitro RNA synthesis and RNA transfection

In vitro synthesis of HCV RNA and RNA transfection were performed as described elsewhere [1].

2.4. Quantification of HCV core protein, luciferase activity, and extra- and intra-cellular infectivity

Quantification of these values was described in Supplementary materials.

2.5. Inhibition of HCV production by a specific NS5A inhibitor

Huh7.5.1 cells (3×10^6) were electroporated with 3 μg of synthetic HCV RNA, suspended in 15 mL complete growth medium, and seeded into 24-well plates. At 4 h after electroporation, the culture medium was replaced with medium containing 0.1% dimethyl sulfoxide (DMSO) with or without various concentrations of the specific NS5A inhibitor BMS-790052 (provided from Bristol-Myers Squibb Company, Plainsboro, NJ) [12]. After 44 h incubation, cells were harvested and HCV core protein was quantified.

2.6. Statistical analysis

Unpaired 2-tailed *t*-test was performed to evaluate the significance of results, and $p < 0.05$ was considered significant.

3. Results

3.1. Development of recombinant HCV with NS5A of genotypes 1 and 2

To establish an HCV cell culture system with NS5A of various strains, we generated recombinant viruses by replacing NS5A of strain JFH-1 with those of genotypes 1 and 2 strains. By transfection of *in vitro* transcribed RNA, efficient production of HCV core protein was detected in JFH-1 wild-type (JFH1/wt) and other recombinant viruses, but not in the replication defective mutant JFH1/GND (Fig. 1A). When compared between JFH1/wt and other recombinant viruses, intracellular core protein levels were comparable at days 2 and 3 after transfection, while extracellular core protein levels were very different. The extracellular core protein level of JFH1/wt-transfected cells increased exponentially up to 23,515 ± 1790 fmol/L at day 3. Similar kinetics was observed in JFH1/5A-H77-transfected cells. However, the extracellular core protein level of JFH1/5A-Con1-transfected cells was approximately 2.5-fold lower than that of JFH1/wt at days 2 and 3. Interestingly, the extracellular core protein levels of intra-genotypic recombinant viruses, JFH1/5A-J6CF and 5A-MA, were 2.5- to 3.5-fold higher than that of JFH1/wt at days 2 and 3. To evaluate the effect of these NS5A replacements on HCV replication, we used recombinant subgenomic reporter replicons, SGR-JFH1/RLuc/wt, 5A-H77, 5A-Con1, 5A-J6CF, and 5A-MA. The *Renilla* luciferase activities of these recombinant subgenomic replicons were comparable to that of SGR-JFH1/Rluc/wt, suggesting similar levels of replication efficiency (Fig. 1B).

To further assess whether NS5A replacement affected other steps of the viral lifecycle, we used a single cycle virus production assay with Huh7-25 cells, a HuH-7-derived cell line lacking CD81 expression on the cell surface [11]. This cell line can support replication and infectious virus production upon transfection of HCV genomic RNA, but cannot be reinfected by produced HCV, therefore allowing the observation of a single cycle of infectious viral production without the confounding effects of reinfection [13]. As shown in Fig. 1C, JFH1/wt yielded an extracellular infectivity titer of 1585 ± 436 FFU/well at day 2 after transfection. JFH1/5A-H77 and 5A-Con1 showed significantly lower titers, while JFH1/5A-J6CF and 5A-MA showed significantly higher intracellular infectivity titers compared to JFH1/wt ($p < 0.05$). These data were consistent with the extracellular core protein levels of JFH1/wt and recombinant viruses (Fig. 1A). A similar tendency was observed in the intracellular infectivity titers of JFH1/wt and recombinant viruses (Fig. 1C). To estimate the efficiency of viral particle assembly, we determined the intracellular specific infectivity by calculating the ratio of the intracellular infectivity titer over the intracellular HCV core protein level. The intracellular specific infectivities of JFH1/5A-H77 and 5A-Con1 were 2.5- and 8-fold lower than that of JFH1/wt, respectively, while JFH1/5A-J6CF and 5A-MA showed 12- and 4-fold higher infectivities compared to JFH1/wt, respectively, suggesting a low assembly efficiency of JFH1/5A-H77 and 5A-Con1, and a high assembly efficiency of JFH1/5A-J6CF and 5A-MA (Fig. 1D). Taken together, all recombinant viruses could replicate and yielded infectious virus. Intra-genotypic recombinant viruses, JFH1/5A-J6CF and 5A-MA, had a higher ability to produce infectious virus than JFH1/wt in cultured cells.

3.2. The C-terminus of NS5A is responsible for enhanced viral assembly

The efficient infectious virus production of intra-genotypic recombinant viruses was unexpected. This prompted us to search for causes of the enhancement. To analyze the enhanced virus assembly of JFH1/5A-J6CF and 5A-MA, we focused on the C-terminus of NS5A of these strains, because this region influence the cleavage between NS5A and NS5B, and the cleavage is reported to be involved in virus assembly [14]. We generated recombinant JFH-1 viruses harboring 10 amino acids of the C-terminus of NS5A of J6CF and MA (JFH1/5AcJ6 and 5AcMA, respectively), and investigated replication and infectious virus production. In these 10 amino acids of the C-terminus of NS5A, JFH1/5AcJ6 and 5AcMA contain 2 and 6 substitutions, respectively, as compared with JFH1/wt, and 2 of them, T2438S and T2439V, are common (Fig. 2A). As shown in Fig. 2B, the extracellular core protein level of JFH1/5AcJ6-transfected cells was higher than those of JFH1/wt- and 5A-J6CF-transfected cells at the examined time points. A similar tendency was observed between JFH1/5AcMA and JFH1/wt or 5A-MA (Fig. 2C). In contrast to the extracellular core protein levels, the intracellular core protein levels were comparable for all NS5A recombinants at the examined time points.

We next assessed the replication of recombinant subgenomic luciferase reporter replicons on the basis of JFH1/5AcJ6 and 5AcMA (Fig. 2D). JFH1/5AcJ6 and 5AcMA showed similar levels of replication to JFH1/wt at day 2 after transfection. To investigate the effects of substitutions at the C-terminus of NS5A on infectious viral particle assembly, we determined the extra- and intracellular infectivity with the single cycle virus production assay with Huh7-25 cells. As shown in Fig. 2E, extra- and intracellular infectivities of